

A Simultaneous Transformation and Rounding Approach for Modeling Integer-Valued Data

Daniel R. Kowal* and Antonio Canale†

March 28, 2022

Abstract

We propose a simple yet powerful framework for modeling integer-valued data. The integer-valued data are modeled by Simultaneously Transforming And Rounding (STAR) a continuous-valued process, where the transformation may be known or learned from the data. Implicitly, STAR formalizes the commonly-applied yet incoherent procedure of (i) transforming integer-valued data and subsequently (ii) modeling the transformed data using Gaussian models. Importantly, STAR is well-defined for integer-valued data, which is reflected in predictive accuracy, and is designed to account for zero-inflation, bounded or censored data, and over- or underdispersion. Efficient computation is available via an MCMC algorithm, which provides a mechanism for direct adaptation of successful Bayesian methods for continuous data to the integer-valued data setting. Using the STAR framework, we develop new linear regression models, additive models, and Bayesian Additive Regression Trees (BART) for integer-valued data, which demonstrate substantial improvements in performance relative to existing regression models for a variety of simulated and real datasets.

KEYWORDS: additive models; BART; count data; nonparametric regression

*Assistant Professor, Department of Statistics, Rice University, Houston, TX (daniel.kowal@rice.edu).

†Assistant Professor, Department of Statistical Sciences, University of Padova, Padova, Italy.

1 Introduction

Integer-valued and count data are ubiquitous in many fields, including epidemiology (Osthus et al., 2018; Kowal, 2019), ecology (Dorazio et al., 2005), and insurance (Bening and Korolev, 2012), among others (Cameron and Trivedi, 2013). Count data also serve as an indicator of demand, such as the demand for medical services (Deb and Trivedi, 1997), emergency medical services (Matteson et al., 2011), and call center access (Shen and Huang, 2008). In these applications and many others, integer-valued data are frequently observed jointly with predictors, over time intervals, or across spatial locations. Integer-valued data also exhibit a variety of distributional features, including zero-inflation, skewness, over- or underdispersion, and in some cases may be bounded or censored. Flexible and interpretable models for *integer-valued processes* are therefore highly useful in practice.

The most widely-used models for count data build upon the Poisson distribution. However, the limitations of the Poisson distribution are well-known: the distribution is not sufficiently flexible in practice and cannot account for zero-inflation or over- and underdispersion. A common strategy is to generalize the Poisson model by introducing additional parameters. Important examples include the quasi-Poisson model (McCullagh and Nelder, 1989), the negative-binomial distribution (Hilbe, 2011), zero-inflated Poisson or negative-binomial models (Cameron and Trivedi, 2013; Neelon et al., 2019), the lognormal Poisson distribution (Zhou et al., 2012), the restricted generalized Poisson distribution (Famoye, 1993), and the Conway-Maxwell Poisson distribution (Lord et al., 2008; Sellers and Shmueli, 2010). A fundamental drawback of these approaches is that the additional degrees of flexibility come at the price of increasing model complexity and difficulties in estimating the additional parameters.

In practice, however, it is exceedingly common for the discrete nature of the data to be ignored. The vast majority of state-of-the-art statistical and machine learning models for

prediction and inference are designed for continuous data. Practitioners often log- or square-root-transform the observed integer-valued data and then directly apply Gaussian methods. For example, Bai et al. (2018) model log-transformed activity counts from wearable device data using a Gaussian functional regression model, while Shen and Huang (2008) forecast square-root-transformed intraday call center counts using techniques for high-dimensional Gaussian time series data. However, transformations to Gaussianity are ineffective for small counts (Warton, 2018), while log-transformations introduce difficulties in the presence of zeros (O’Hara and Kotze, 2010). More broadly, these approaches are not well-defined for integer-valued data: the data-generating process for a (transformed) Gaussian model cannot produce discrete data, which immediately amplifies model misspecification, limits interpretability, and undermines the reliability of inference and predictive distributions.

To address these challenges, we propose a coherent modeling framework for integer-valued data. The process is defined by *simultaneously transforming and rounding* (STAR) a continuous-valued process. Specifically, STAR defines an integer-valued data-generating process as follows. First, a *continuous-valued process* is specified to model the dependence between (latent) variables. We focus on conditionally Gaussian models, but the STAR framework applies more broadly. Second, the latent variables are *transformed* for greater distributional flexibility. The transformation may be specified in advance or learned from the data. Lastly, the transformed latent variables are filtered through a *rounding operator* mapping them to the (nonnegative) integers. This construction is designed to mimic the popular approach of transforming count data and applying Gaussian models, such as Bai et al. (2018) and Shen and Huang (2008), yet produces a well-defined integer-valued process. Importantly, we show that STAR processes are sufficiently flexible to account for zero-inflation, bounded or censored data, and over- or underdispersion.

A major benefit of the proposed approach is its computational modularity for Bayesian inference: using a simple and efficient data augmentation technique, existing computational

tools for Bayesian inference under continuous data models can be used for Bayesian inference under STAR models. As a result, STAR provides a cohesive framework for seamlessly adapting state-of-the-art continuous data models and algorithms to the integer-valued data setting. Using this construction, we develop new models for linear regression, additive models, and Bayesian additive regression trees (Chipman et al., 2010) for integer-valued data. These new models are applied to medical demand estimation and animal population modeling, and further evaluated using additional real and simulated datasets. The STAR models demonstrate exceptional empirical performance with substantial improvements over existing methods.

The remainder of the paper is organized as follows. Section 2 introduces the STAR model, provides parametric and nonparametric specifications for the (known or unknown) transformation, describes important properties, and discusses computational details for posterior inference. Section 3 provides example STAR models, which are applied to simulated and real datasets in Sections 4 and 5, respectively; Section 6 concludes. Additional simulation results and further empirical comparisons in the Appendix. Methods are implemented in the R package `rSTAR` available on GitHub.

2 Simultaneously Transforming And Rounding

Consider a count-valued stochastic process $y: \mathcal{X} \rightarrow \mathcal{N}$, where \mathcal{X} may correspond to predictors, times, or spatial locations and $\mathcal{N} = \{0, \dots, \infty\}$. Although we focus on the nonnegative integers, our procedure may be trivially modified for integer-valued data and rounded data. We are interested in constructing a joint probability distribution for y that simultaneously builds upon successful approaches for continuous stochastic processes (observed on \mathbb{R} or \mathbb{R}^+), yet is well-defined on \mathcal{N} .

To this end, we first introduce continuous-valued process $y^*: \mathcal{X} \rightarrow \mathcal{T}$, $\mathcal{T} \subseteq \mathbb{R}$ related to

the observed count-valued data y via

$$y = h(y^*), \tag{1}$$

where $h: \mathcal{T} \rightarrow \mathcal{N}$ is a *rounding* operator that sets $y(x) = j$ when $y^*(x) \in \mathcal{A}_j$ and $\{\mathcal{A}_j\}_{j=0}^\infty$ is a known partition of \mathcal{T} . For example, we may use the floor function defined by $\mathcal{A}_j = [a_j, a_{j+1}) = [j, j + 1)$ for $j \in \mathcal{N}$; modifications are available for zero-inflated, bounded, or censored data (see Section 2.2). Naturally, the properties of the count-valued process y will be determined by the rounding operator h and the distribution of the continuous-valued process y^* . Previous approaches for modeling y^* include nonparametric mixtures of kernels (Canale and Dunson, 2011) and Gaussian processes (Canale and Dunson, 2013). We propose to induce a distribution on y^* by *transforming* y^* and specifying a distribution Π_θ on the transformed scale:

$$g(y^*) = z^*, \quad z^* \sim \Pi_\theta, \tag{2}$$

where $g: \mathcal{T} \rightarrow \mathbb{R}$ is a (known or unknown) strictly monotone function.

Equations (1)-(2) constitute the core of the *simultaneously transforming and rounding* (STAR) model that will be denoted henceforth by $\text{STAR}(h, g, \Pi_\theta)$. The process y^* operates as a continuous proxy for the observed integers y , which is more convenient for modeling, yet has a simple mapping to the observable count-valued process y in (1). The proxy y^* is then transformed and modeled via (2), akin to the common practice of log- or square-root transforming count data prior to application of continuous (Gaussian) models. In this paper, we focus on the assumption that Π_θ , the joint probability of z^* , is a *conditionally Gaussian* model, which can incorporate a variety of commonly-used models, such as linear regressions, mixed effects models, spatio-temporal models, ARIMA models, Gaussian processes, and other nonparametric regression techniques. However, the STAR framework is sufficiently general to incorporate any continuous family of stochastic process for the latent z^* .

An important special case of (2) is the “signal-plus-noise” model, i.e.

$$z^*(x) = \mu(x) + \epsilon(x), \quad \epsilon(x) \stackrel{\text{indep}}{\sim} N(0, \sigma^2(x)), \quad (3)$$

where $\mu(x)$ is the conditional expectation of $z^*(x)$ and the errors $\epsilon(x)$ are independent but possibly heteroscedastic, conditional on $x \in \mathcal{X}$. Given the wide success and simplicity of (3), we will mainly focus on this specification in the remainder of the article. Examples of (3) include linear regression models with $\mu(x) = x'\beta$ as well as more sophisticated nonparametric regression models such as additive models or BART (Chipman et al., 2010). We implement each of these models for simulated and real count data in Sections 4 and 5, respectively.

The distribution of y is completely determined by the rounding operator h , the transformation g , and the distribution Π_θ . Specifically, the probability mass associated to $y(x) = j$ for each integer $j \in \mathcal{N}$ is

$$\mathbb{P}\{y(x) = j\} = \mathbb{P}\{y^*(x) \in \mathcal{A}_j\} = \mathbb{P}\{z^*(x) \in g(\mathcal{A}_j)\}. \quad (4)$$

The distribution of z^* is given by Π_θ , while $g(\mathcal{A}_j)$ is determined by the transformation g and the rounding operator h . For model (3) and $\mathcal{A}_j = [a_j, a_{j+1})$, the probability mass function (4) simplifies to

$$\mathbb{P}\{y(x) = j\} = \Phi\left(\frac{g(a_{j+1}) - \mu(x)}{\sigma(x)}\right) - \Phi\left(\frac{g(a_j) - \mu(x)}{\sigma(x)}\right). \quad (5)$$

The distribution in (5) is related to, yet distinct from, ordinal regression (McCullagh, 1980). In ordinal regression, each term $g(a_j)$ in (5) is replaced by an unknown latent threshold, say ω_j , with an ordering constraint $\omega_j \leq \omega_{j+1}$ for all j . However, the latent thresholds ω_j are based only on the *ranks* of the observed data, and therefore ignore the information contained in the numeric values of the observed counts. Furthermore, since each threshold ω_j

is unknown, ordinal regression introduces a new parameter for each unique data value, and therefore produces a heavily-parametrized model that is challenging to estimate. By comparison, STAR is substantially more parsimonious: if g is known, no new parameters are needed, while if g is unknown, only a small number of parameters are needed (see Section 2.1).

The STAR approach is fundamentally different from simply rounding the predictions from a continuous data model such as (2) or (3). In particular, such a *post hoc* rounding procedure ignores the discrete nature of the data in model-fitting. Critically, *post hoc* rounding introduces a disconnect between the *fitted model* and the model used for *prediction*. STAR clearly avoids this issue, and maintains the benefits of incorporating widely-used models for continuous data while producing a coherent integer-valued predictive distribution.

2.1 The transformation g

The transformation g is a crucial component of STAR. When $g(t) = t$ and z^* is a draw from a Gaussian process, STAR simplifies to the rounded Gaussian process model of Canale and Dunson (2013). However, the identity transformation is likely suboptimal in many cases. First, the popularity of log-linear models for count data, especially Poisson and negative-binomial models, suggests that regression effects $\mu(x)$ are often multiplicative for count data, and that the log-transformation $g(t) = \log(t)$ may be preferable for many applications. Similarly, the square-root transformation $g(t) = \sqrt{t}$ is the variance-stabilizing transformation of the Poisson distribution, and therefore is a common choice in applications of Gaussian methods to transformed count data. Empirically, the simulation studies and real data analyses in Sections 4 and 5, respectively, demonstrate that the transformation g provides substantial improvements in modeling flexibility and accuracy relative to the untransformed approach of Canale and Dunson (2013).

When g is fixed and known, the only unknowns in STAR are the parameters θ in the distribution Π_θ of the latent data z^* in (2). This setting is most similar to the popular

approach of transforming count data and applying Gaussian models, yet produces a coherent integer-valued process. A fixed transformation g shares some characteristics with the link function of a generalized linear model (GLM) (McCullagh and Nelder, 1989). In the GLM framework, the link function maps the expectation of an exponential family distribution to \mathbb{R} so that, conditional on this transformation, the expectation can be modeled using a linear predictor. For STAR, g maps the continuous-valued y^* to \mathbb{R} and under (3) models the conditional expectation of the latent variable z^* using $\mu(x)$.

For general application of STAR, pre-specification of a transformation g may be restrictive. By allowing the data to determine the transformation g , the implied distribution for y becomes more flexible, and the risk of model misspecification is lessened. In the context of GLMs, Mallick and Gelfand (1994) similarly relax the assumption of a known link function, adopting a nonparametric approach. In our setting, we require that the functions g satisfy the following important properties: (i) *monotonicity*, which preserves the ordering of the observed integers in the transformed latent space; (ii) *smoothness*, which provides regularization by encouraging information-sharing among nearby values; and (iii) *shrinkage* toward a pre-specified transformation, such as log or square-root. We consider both parametric and nonparametric models for g , which are comparatively evaluated using simulated and real data in Sections 4 and 5, respectively.

A natural parametric specification for g satisfying the aforementioned criteria is the (signed) *Box-Cox* transformation (Box and Cox, 1964), i.e.

$$g(t; \lambda) = \frac{\text{sgn}(t)|t|^\lambda - 1}{\lambda}, \quad \lambda > 0, \quad (6)$$

with $g(t; \lambda = 0) = \log(t)$. Box-Cox functions are a popular choice for transforming continuous data towards Gaussianity, which in the present setting is similar to (2) when Π_θ is Gaussian. Important special cases of (6) include the (shifted) identity transformation $g(t; \lambda = 1) = t - 1$,

the (shifted and scaled) square-root transformation $g(t; \lambda = 1/2) = 2\sqrt{|t|} - 2$, and the log-transformation. Note that we define (6) on the real line, but typically the inputs will be nonnegative. Under a Bayesian approach, a prior distribution for λ is necessary to learn the shape of the transformation g from the data. As a default choice we recommend the prior $\lambda \sim N(1/2, 1)$ truncated to $[0, 3]$, which shrinks g toward the (shifted and scaled) square-root transformation.

For greater flexibility, we also consider fully nonparametric specification for g . To enforce monotonicity and smoothness, we represent g using an I-spline basis expansion (Ramsay, 1988):

$$g(t) = b'_I(t)\gamma, \tag{7}$$

where b_I is an L -dimensional vector of I-spline basis functions and γ are the unknown basis coefficients. Since each I-spline basis function is monotone increasing, we ensure monotonicity of g by restricting the elements of γ to be positive. Note that a nonparametric model for g is distinct from a nonparametric model for the probability mass function of the count data, such as a Dirichlet process (Ferguson, 1973; Carota and Parmigiani, 2002), nonparametric mixtures of discrete (e.g., Poisson) kernels, or nonparametric mixtures of rounded Gaussian kernels (Canale and Dunson, 2011).

We propose a prior for γ in (7) that simultaneously enforces monotonicity, smoothness, and shrinkage toward a pre-specified transformation. However, care must be taken to ensure identifiability of the STAR model and retain interpretability of the parameters θ in Π_θ . In particular for model (3), arbitrary shifting and scaling of g can be matched by shifting and scaling of μ and σ . The parametric transformation (6) preserves identifiability: $g(1, \lambda) = 0$ for all λ (shift constraint) and the prior on λ is weakly informative (scale constraint). For nonparametric g in (7), we resolve the identifiability issue by fixing $g(0) = 0$ (shift constraint), which is satisfied automatically due to the I-spline construction, and $\lim_{t \rightarrow \infty} g(t) = 1$ (scale

constraint), which is enforced by constraining $\sum_{\ell=1}^L \gamma_\ell = 1$. Specifically, let

$$\gamma_\ell = \tilde{\gamma}_\ell / \sum_{k=1}^L \tilde{\gamma}_k, \quad \tilde{\gamma}_\ell \overset{\text{indep}}{\sim} N_+(\mu_{\gamma_\ell}, \sigma_\gamma^2), \quad \ell = 1, \dots, L, \quad (8)$$

where N_+ is the half-normal distribution. Clearly, $\gamma_\ell > 0$ for each ℓ and $\sum_{\ell=1}^L \gamma_\ell = 1$, which guarantees monotonicity of g and preserves identifiability of model (3). We select the prior mean $\mu_\gamma = (\mu_{\gamma_1}, \dots, \mu_{\gamma_L})'$ such that $g(t)$ is *a priori* centered around a parametric function of interest, such as (6) with fixed $\lambda = \lambda_0$, and model σ_γ^2 with an inverse-Gamma prior to allow the data to determine the amount of shrinkage toward the parametric function of interest. Let $\mathbf{t}_g = (0, 1, \dots, a_{\max y_i + 1})'$ and let B_I be the I-spline basis evaluated at \mathbf{t}_g , so $g(\mathbf{t}_g) = B_I \mu_\gamma$. We solve $\tilde{\mu}_\gamma = \arg \min_{\mu_\gamma} \|g(\mathbf{t}_g; \lambda_0) - B_I \mu_\gamma\|^2$ subject to $\tilde{\mu}_{\gamma_\ell} > 0$ for $\ell = 1, \dots, L$, which is a one-time cost, and normalize $\mu_{\gamma_\ell} = \tilde{\mu}_{\gamma_\ell} / \sum_{k=1}^L \tilde{\mu}_{\gamma_k}$. In the simulations and applications of Sections 4 and 5, we fix $\lambda_0 = 1/2$ and model $\sigma_\gamma^{-2} \sim \text{Gamma}(0.001, 0.001)$.

For the I-spline basis, we use quadratic splines with $L = 2 + \min\{\lceil \# \text{ unique } y_i \rceil / 4, 10\}$ knots, implemented using the `splines2` package in R (Wang and Yan, 2018). Boundary knots are placed at zero and $\max\{y_i\}$, while the $L - 2$ interior knots selected using the sample quantiles of $\{y_i\}$ excluding zero, one, and $\max\{y_i\}$, with an interior knot placed at one to improve distributional flexibility near zero. Note that Ramsay (1988) use $L = 3$ or $L = 5$ in all monotone spline examples, which suggests that a small number of knots may be adequate in many cases.

2.2 Properties

By design, STAR builds upon models for continuous data, such as those in Section 3, and adapts them for integer-valued data. Yet STAR is not merely a mechanism for producing valid integer-valued processes: STAR also provides important distributional properties for modeling integer-valued data in practice. By careful selection of the rounding operator h

and the transformation g , STAR provides the capability to model zero-inflation, bounded or censored data, and over- or underdispersion.

In applications with count data, it is common to observe an abundance of zeros, $y(x) = 0$. STAR can be parametrized such that zero counts occur whenever the continuous-valued process z^* is negative:

Lemma 1 (Zero-inflation). *For any STAR model with $g(\mathcal{A}_0) = (-\infty, 0)$, we have (i) $y(x) = 0$ if and only if $z^*(x) < 0$ and (ii) $\mathbb{P}\{y(x) = 0\} = \mathbb{P}\{z^*(x) \leq 0\}$.*

Lemma 1 is valid for known or unknown transformations, and is easily satisfied for (6) letting $\mathcal{A}_0 = (a_0, a_1) = (-\infty, 1)$ for $\lambda \neq 0$ and $\mathcal{A}_0 = (a_0, a_1) = (0, 1)$ for $\lambda = 0$. For model (3), Π_θ is conditionally Gaussian, which may place substantial prior mass on $z^*(x) < 0$ and thus $y(x) = 0$. Therefore, STAR has a built-in and interpretable mechanism for handling zero counts, and does not require the addition of an artificial constant to the transformation, such as $\log(y + 1)$. Furthermore, dependence among zero values is implicit in the model: $\mathbb{P}\{y(x) = 0, y(x') = 0\} = \mathbb{P}\{z^*(x) < 0, z^*(x') < 0\}$ depends on the joint distribution of $(z^*(x), z^*(x'))$, which is modeled by Π_θ .

Another common characteristic of count-valued data is a deterministic upper bound K . For instance, if y counts the number of days on which an event occurred in a given year, then $y(x) \in \{0, 1, \dots, K\}$ and $K = 365$. STAR can easily incorporate this information into the distribution for y as formalized in the next lemma.

Lemma 2 (Bounded observations). *For any STAR model, letting $g(\mathcal{A}_K) = [g(a_K), \infty)$ implies $\mathbb{P}\{y(x) \leq K\} = 1$.*

The boundedness constraints in Lemma 2 are compatible with any choice of (unconstrained) continuous-valued model (2) and do not require modification of the algorithms for estimation and inference in Section 2.3. Similar to the case of zero values in Lemma 1, STAR allows for dependence among y values that attain the upper bound: $\mathbb{P}\{y(x) = K, y(x') =$

$K\} = \mathbb{P}\{z^*(x) \geq g(a_K), z^*(x') \geq g(a_K)\}$, which again is modeled by (2) or (3). When $K = 1$, the STAR model (3) with $\mu(x) = x'\beta$ and $\sigma^2(x) = 1$ simplifies to probit regression.

Interestingly, the construction in Lemma 2 is coherent under right-censoring, which occurs when an observed count value of K implies that $y(x) \geq K$. Right-censoring is common in surveys, where large values are often grouped together. The following lemma formalizes the properties of STAR subject to right-censoring of the observations.

Lemma 3 (Right-censoring). *For right-censored observations $y_c(x) = \min\{y(x), K\}$ with $y \sim \text{STAR}(h, g, \Pi_\theta)$ and $y_c \sim \text{STAR}(h', g, \Pi_\theta)$ such that h and h' satisfy $a_K = a'_K$ and $\mathcal{A}'_K = [a_K, \infty)$, we have $\mathbb{P}\{y(x) \geq K\} = \mathbb{P}\{z^*(x) \geq g(a_K)\} = \mathbb{P}\{y_c(x) = K\}$.*

For right-censored data, the likelihood includes terms of the form $\mathbb{P}\{y(x) \geq K\}$ for censored observations. Lemma 3 shows that the censored likelihood terms under a STAR model for y are equivalent to the non-censored likelihood terms $\mathbb{P}\{y_c(x) = K\}$ under a STAR model for $y_c = \min\{y(x), K\}$ with $\mathcal{A}'_K = [a_K, \infty)$. Remarkably, STAR preserves the correct right-censored likelihood for y by directly modeling the observed counts y_c and setting $\mathcal{A}'_K = [a_K, \infty)$, with no further modifications needed for the model specification or estimation procedure. By comparison, common parametric approaches for modeling count data, such as the Poisson model and its generalizations, require careful modifications of the likelihood and tailored algorithms for estimation and inference in the case of right-censoring. Naturally, a similar approach is available for left-censoring.

Lastly, we note that STAR processes are capable of modeling over- or underdispersion. In Figure 1, we illustrate the relationships among the expectation $\mathbb{E}[y]$, the variance $\text{Var}(y)$, and the probability of zeros $\mathbb{P}(y = 0)$ for a STAR process defined by $z^* \sim N(\mu, \sigma^2)$ and transformation (6) with $\lambda = 1/2$. For different values of the parameters the STAR process exhibits different features, including overdispersion, underdispersion, and zero-inflation.

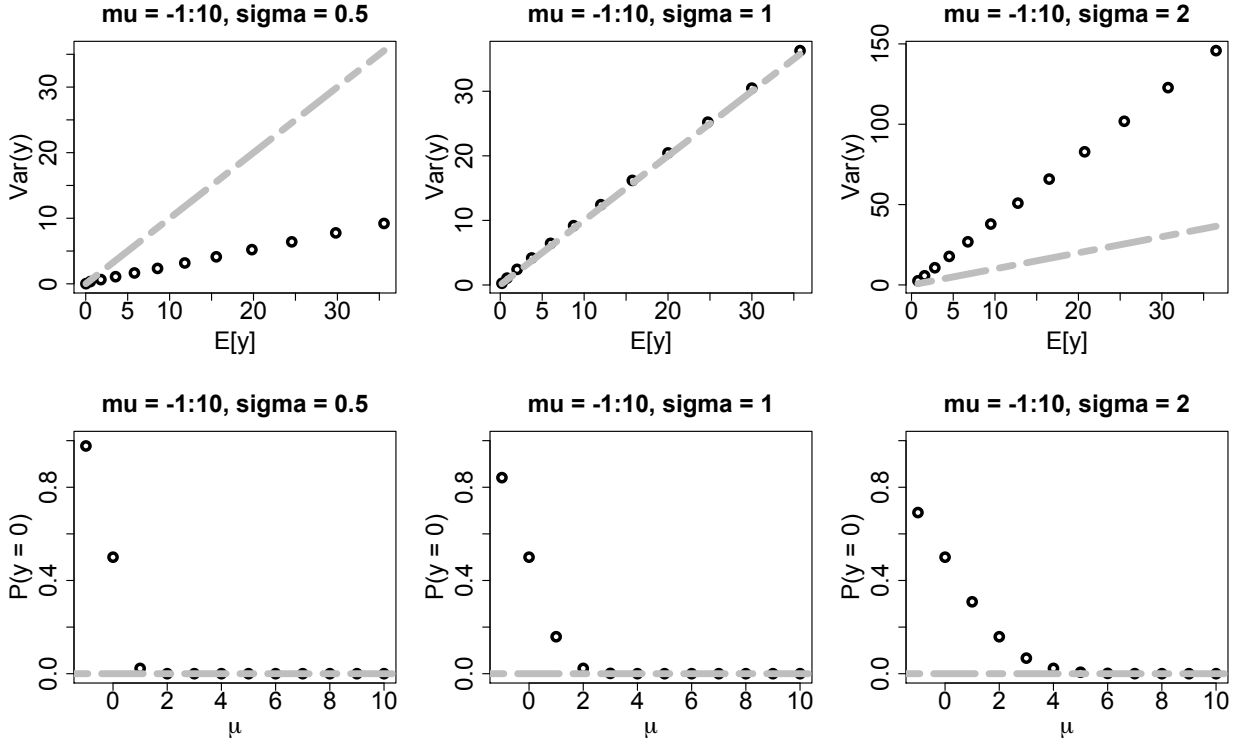


Figure 1: $\mathbb{E}[y]$ and $\text{Var}(y)$ (top) and $\mathbb{P}(y = 0)$ (bottom) for a STAR process defined by $z^* \sim N(\mu, \sigma^2)$ and transformation (6) with $\lambda = 1/2$ for various (μ, σ) pairings. The dashed gray lines corresponds to $\mathbb{E}[y] = \text{Var}(y)$ (top) and $\mathbb{P}(y = 0) = 0$ (bottom). STAR processes may include underdispersion (top left), overdispersion (top right), and zero-inflation (bottom).

2.3 Posterior inference

We develop a general Markov Chain Monte Carlo (MCMC) algorithm for Bayesian inference under STAR. The hierarchical construction of STAR in (1)-(2) is accompanied by a computationally convenient data augmentation strategy, which we leverage to incorporate existing sampling techniques for the unknown parameters θ in (2). To emphasize the modularity of the proposed approach, we omit model-specific details for sampling θ until Section 3.

Let $\mathcal{D} = \{x_i, y_i\}_{i=1}^n$ denote the observed pairs of points $x_i \in \mathcal{X}$ and integer-valued data $y_i = y(x_i)$. Consider a Bayesian specification of (2) with suitable prior on θ and an algorithm \mathbb{A} which draws from the posterior distribution of θ given the (continuous) data. The sampling

algorithm \mathbb{A} is designed for continuous data, such as linear regressions, additive models, or BART, depending on the different choices for Π_θ (see Section 3 for details). The posterior sampling algorithm for STAR defines a Gibbs sampler by combining a data augmentation step with algorithm \mathbb{A} as follows:

1. Sample $[z^*(x_i) \mid \mathcal{D}, \theta]$ from Π_θ truncated to $z^*(x_i) \in g(\mathcal{A}_{y_i})$ for $i = 1, \dots, n$;
2. Sample $[\theta \mid \mathbf{z}^*]$ using algorithm \mathbb{A} conditioning on $\mathbf{z}^* = (z^*(x_1), \dots, z^*(x_n))'$.

In the case of model (3), the data augmentation step may be computed efficiently using a standard univariate truncated normal sampler. Specifically, for $\mathcal{A}_j = [a_j, a_{j+1})$, the full conditional distribution of the latent data is $[z^*(x_i) \mid \mathcal{D}, \theta] \sim N(\mu(x_i), \sigma^2(x_i))$ truncated to $[g(a_{y_i}), g(a_{y_i+1}))$. Note that while the process y^* is useful for interpretability of the STAR model, it is not necessary for inference or sampling.

When the transformation g is unknown, an additional sampling step is required. For the parametric Box-Cox case (6) this translates to sampling the parameter λ from its full conditional posterior distribution, for which we use a slice sampler (Neal, 2003). For the nonparametric model (7) with prior (8), we sample $\xi_\gamma = \log(\tilde{\gamma})$ using Metropolis-Hastings and $[\sigma_\gamma^{-2} \mid -] \sim \text{Gamma}\{0.001 + L/2, 0.001 + \sum_{\ell=1}^L (\tilde{\gamma}_\ell - \mu_{\gamma_\ell})^2\}$, and set $g(t) = b'_I(t)\gamma$ as defined in (7)-(8). For sampling ξ_γ , we employ a Gaussian random walk proposal and tune the covariance matrix using the robust adaptive Metropolis (RAM) algorithm of Vihola (2012) during a preliminary burn-in period. Within the RAM algorithm we set a target acceptance rate of 30% with an adaptation rate of 0.75; see Vihola (2012) for details. We adapt the proposal covariance only during the first 50% of the burn-in period, so the MCMC draws we save for inference are generated from a (non-adaptive) Metropolis-within-Gibbs sampling algorithm.

To simulate from the posterior predictive distribution $[\tilde{y}(x) \mid \mathcal{D}]$, we incorporate one additional step: sample $[\tilde{z}^*(x) \mid \theta]$ from Π_θ using the current draw of θ and set $\tilde{y}(x) =$

$h[g^{-1}\{\tilde{z}^*(x)\}]$ for each x . This additional step is extremely simple, yet provides (i) inference for count-valued predictions and forecasts, (ii) important model diagnostics (see Section 5), and (iii) a model-based approach for imputing missing data at $x \in \mathcal{X}$. For parametric g in (6), the functions $g^{-1}(s; \lambda)$ are known, while for nonparametric g we approximate $g^{-1}(s) \approx \arg \min_t |s - b'_I(t)\gamma|$, where the minimum t is computed over a grid of values.

The proposed framework for MCMC balances modularity and flexibility: it combines existing algorithms for continuous or Gaussian models with a transformation to provide distributional flexibility for integer-valued data. The importance of modularity has been demonstrated recently for the negative-binomial distribution, for which Polson et al. (2013) developed a Pólya-Gamma data augmentation scheme for Gibbs sampling. This approach has allowed a variety of Gaussian models to be extended for negative-binomial data, including linear regression (Zhou et al., 2012), factor models (Klami, 2015), and functional time series models (Kowal, 2019), yet faces two important limitations: first, it is restricted to the negative-binomial distribution, and second, the resulting MCMC sampler is often inefficient (Duan et al., 2018). From our experience, the proposed STAR algorithm provides excellent MCMC efficiency in the simulations and applications considered in Sections 4 and 5 (see the Appendix for empirical validation).

3 Specific examples

To illustrate the modularity and modeling flexibility provided by STAR, we consider three classes of models that have proven successful for Gaussian data: linear regressions (Section 3.1), additive models (Section 3.2), and BART (Section 3.3). Each model may be combined with a known or unknown transformation as discussed in Section 2.1. These examples, with various transformations, are applied in Sections 4 and 5.

3.1 Linear regression

The simplest and most common special case of (3) is linear regression, where $\sigma^2(x) = \sigma^2$ and $\mu(x) = x'\beta$ for x a p -dimensional vector of predictors. Let X denote the $n \times p$ matrix of predictors, and consider the (independent) priors $[\beta] \sim N(0, \Sigma_\beta)$ and $[\sigma^{-2}] \sim \text{Gamma}(a_\sigma, b_\sigma)$, where Σ_β is the prior covariance for the regression coefficients. We focus on the ridge prior $[\beta_j | \sigma_\beta] \stackrel{iid}{\sim} N(0, \sigma_\beta^2)$ for illustration, with $[\sigma_\beta] \sim \text{Uniform}(0, A)$, but extensions for other shrinkage priors are available (Carvalho et al., 2010). The Gibbs sampler for the STAR linear model is given by the following steps:

1. Sample $[z^*(x_i) | -] \sim N(x'_i\beta, \sigma^2)$ truncated to $z^*(x_i) \in g(\mathcal{A}_{y_i})$ for $i = 1, \dots, n$;
2. Sample $[\beta | -] \sim N(Q_\beta^{-1}\ell_\beta, Q_\beta^{-1})$ where $Q_\beta = \sigma^{-2}X'X + \Sigma_\beta^{-1}$ and $\ell_\beta = \sigma^{-2}X'z^*$;
3. Sample $[\sigma^{-2} | -] \sim \text{Gamma}[a_\sigma + n/2, b_\sigma + \sum_{i=1}^n \{z^*(x_i) - x'_i\beta\}^2/2]$;
4. Sample $[\sigma_\beta^{-2} | -] \sim \text{Gamma}\{(p-1)/2, \sum_{j=1}^p \beta_j^2\}$ truncated to $[1/A^2, 0)$ and set $\Sigma_\beta = \sigma_\beta^2 I_p$.

For other conditionally Gaussian shrinkage priors, only the sampler for $[\Sigma_\beta | -]$ in the final step must be modified. Note that we include a diffuse prior on the intercept, $\beta_0 \sim N(0, 10^6)$, and select the hyperparameters $a_\sigma = b_\sigma = 0.001$ and $A = 10^4$ for Sections 4 and 5.

Computational scalability of the STAR linear model is primarily determined by the sampler for the regression coefficients β , which depends on both the sample size n and the number of predictors p . Importantly, computationally efficient samplers for $[\beta | z^*, \sigma^2]$ exist for $p < n$ (Rue, 2001) and $p \gg n$ (Bhattacharya et al., 2016) for conditionally Gaussian priors. By design, the STAR MCMC algorithm leverages these existing priors and algorithms for Gaussian data to provide efficient and scalable posterior inference for integer-valued data.

3.2 Additive models

Relaxing the linearity assumptions of Section 3.1, consider an additive model for (3):

$$\mu(x) = u'\beta + \sum_j f_j(v_j), \quad (9)$$

where the predictors $x' = (u', v')$ are partitioned into linear predictors u and nonlinear predictors v , and $f_j: \mathcal{X}_j \rightarrow \mathbb{R}$ is an unknown function of $v_j \in \mathcal{X}_j$. The unknown functions f_j are typically modeled as smooth nonparametric functions, and therefore may capture nonlinearities in each variable v_j .

As in the case of the STAR linear model, we build upon successful model parametrizations, prior distributions, and sampling algorithms previously utilized for Gaussian data. The linear regression coefficients in (9) are given conditionally Gaussian priors, $\beta \sim N(0, \Sigma_\beta)$ as in Section 3.1. The nonlinear functions in (9) are modeled smoothly using a basis expansion $f_j(v_j) = b_j'(v_j)\alpha_j$, where b_j is a L_j -dimensional vector of low-rank thin plate splines and α_j is a vector of unknown coefficients. Thin plate splines are flexible, computationally efficient, and well-defined for $\mathcal{X}_j \in \mathbb{R}^d$ with $d = 1, 2, 3, \dots$, for example if v_j is a two-dimensional spatial location (Crainiceanu et al., 2005). We assume a smoothness prior on f_j , which may be diagonalized and represented via $\alpha_j \overset{indep}{\sim} N(0, \sigma_{f_j}^2 I_{L_j})$ (Wand and Ormerod, 2008). For identifiability, we constrain each function f_j such that $\sum_{i=1}^n f_j(v_{i,j}) = 0$, enforced by a simple reparametrization of the basis b_j (Wood, 2006). As in Section 3.1, we employ conditionally conjugate priors on the precisions: $\sigma^{-2} \sim \text{Gamma}(0.001, 0.001)$ and $\sigma_{f_j}^{-2} \sim \text{Gamma}(0.1, 0.1)$.

For observed predictors $x'_i = (u'_i, v'_i)$, let U denote the matrix of linear predictors and let $\mathbf{f}_j = B_j\alpha_j$ denote the nonlinear function f_j evaluated at all observation points $\{v_{i,j}\}_{i=1}^n$ with basis matrix B_j . The Gibbs sampler for the STAR additive model iterates the following full conditional distributions:

1. Sample $[z^*(x_i) \mid -] \sim N(u'_i\beta + \sum_j f_j(v_{i,j}), \sigma^2)$ truncated to $z^*(x_i) \in g(\mathcal{A}_{y_i})$;

2. Sample $[\beta \mid -] \sim N(Q_\beta^{-1}\ell_\beta, Q_\beta^{-1})$ where $Q_\beta = \sigma^{-2}U'U + \Sigma_\beta^{-1}$ and $\ell_\beta = \sigma^{-2}U'(\mathbf{z}^* - \sum_j \mathbf{f}_j)$;
3. For each j , sample $[\alpha_j \mid -] \sim N(Q_{\alpha_j}^{-1}\ell_{\alpha_j}, Q_{\alpha_j}^{-1})$ where $Q_{\alpha_j} = \sigma^{-2}B'_jB_j + \sigma_{\alpha_j}^{-2}I_{L_j}$ and $\ell_{\alpha_j} = \sigma^{-2}B'_j(\mathbf{z}^* - U\beta - \sum_{k \neq j} \mathbf{f}_k)$ and set $\mathbf{f}_j = B_j\alpha_j$;
4. Sample $[\sigma^{-2} \mid -] \sim \text{Gamma}(0.001 + n/2, 0.001 + \|\mathbf{z}^* - U\beta - \sum_j \mathbf{f}_j\|^2/2)$;
5. For each j , sample $[\sigma_{\alpha_j}^{-2} \mid -] \sim \text{Gamma}(0.1 + L_j/2, 0.1 + \sum_{\ell=1}^{L_j} \alpha_j^2/2)$.

Additional sampling steps for Σ_β proceed as in Section 3.1. Note that since each $f_j(v_j)$ includes a linear effect in v_j , which is typically unpenalized by the smoothness prior for f_j , we group these linear terms with u and sample all of the linear coefficients for x jointly.

3.3 Bayesian Additive Regression Trees

While additive models are effective at capturing nonlinear marginal effects, they are often inadequate for modeling interactions among predictors. Specific pairwise or higher order interactions may be specified in advance, but including all possible interactions in an additive model requires a massive number of parameters. As a remedy, Chipman et al. (2010) proposed BART, which is a “sum-of-trees” model within a fully Bayesian framework. Tree-based regression models, such as Chipman et al. (1998), are designed to model complex interactions among predictors. Notably, BART utilizes many trees, where each individual tree is constrained via the prior to be a weak learner. As a result, BART provides the capability to capture nonlinear interactions yet features built-in mechanisms to guard against overfitting. For continuous and binary data, the predictive performance of BART is highly competitive with state-of-the-art statistical and machine learning models.

For integer-valued data, BART has been relatively underutilized. Adaptations of BART for negative-binomial data are feasible via Pólya-Gamma augmentation (Polson et al., 2013),

similar to the probit implementation in Chipman et al. (2010) for binary data. However, this approach is limited in distributional flexibility, and the MCMC inefficiencies of Pólya-Gamma augmentation are unlikely to be ameliorated given the complexity of the (Gaussian) BART sampling algorithm. Recently, Murray (2017) proposed a log-linear BART model for count-valued and categorical data. The accompanying MCMC algorithm utilizes a parameter expansion valid for certain likelihoods in log-linear models, in particular (zero-inflated) negative-binomial and Poisson. However, extensions to more flexible count distributions may require alternative computational strategies. Furthermore, Murray (2017) requires a new set of prior distributions with hyperparameters that are distinct from those in Chipman et al. (2010). Due to the wide application of BART, the effects of the priors and hyperparameters in Chipman et al. (2010) are relatively well-known, with default values often providing exceptional performance. A key feature of STAR is that, by transforming to Gaussianity, we inherit the same framework as the original BART, and therefore may directly incorporate those priors and hyperparameters. In addition, as new BART modifications and priors are proposed for continuous data, such as variable selection techniques (Linero, 2018) and smoothness priors (Linero and Yang, 2018), STAR provides a framework for directly adapting these methods to integer-valued data.

Within the STAR framework, we parametrize the BART model (BART-STAR) as in Chipman et al. (2010) and specifically

$$\mu(x) = \sum_{k=1}^m f(x; T_k, M_k), \quad (10)$$

where T_k is a binary tree comprised of interior splitting rules and terminal nodes and $M_k = \{\eta_{1,k}, \dots, \eta_{b_k,k}\}$ is the value at each of b_k terminal nodes for tree T_k . For a given predictor x , each tree T_k in (10) assigns a value $\eta_{\ell,k} \in M_k$, and these values are summed across all trees $k = 1, \dots, m$. Chipman et al. (2010) propose prior distributions that (i) constrain each T_k to be shallow, thereby limiting the order of interactions, and (ii) constrain each $\eta_{\ell,k}$ to

be small, thereby limiting the contribution of each tree. Both mechanisms guard against overfitting, and in combination produce a sum of weak learners. The joint prior distribution is specified as a prior for the tree, $p(T_k)$, which follows Chipman et al. (1998), and a prior for the terminal values given the tree, $p(\eta_{\ell,k}|T_k)$, which is Gaussian. For Sections 4 and 5, we adopt the default priors and hyperparameters suggested by Chipman et al. (2010).

More careful consideration is required for the prior distribution of the error variance σ^2 . Chipman et al. (2010) emphasize that an informative prior distribution is important to balance between overly aggressive and overly conservative model fits. In particular, Chipman et al. (2010) parametrize the prior for σ^2 as an inverse chi-square distribution calibrated using a data-based overestimate $\hat{\sigma}$ of σ . However, any statistics calculated from the raw count-valued data are likely inappropriate for STAR, since the (possibly unknown) transformation g impacts the scale of z^* . As a remedy, we compute $\hat{\sigma}$ as the posterior median of σ from the STAR linear model in Section 3.1, where the transformation in the linear model is chosen to match the transformation in BART-STAR. Given $\hat{\sigma}$, which indeed is a data-based overestimate of σ , we adopt the default hyperparameter suggestions of Chipman et al. (2010).

For posterior inference under BART-STAR, we combine a data augmentation step for $z^*(x_i)$ similar to Sections 3.1 and 3.2 with a sweep from the original Chipman et al. (2010) algorithm to draw the BART parameters in (10) using z^* as data. The Chipman et al. (2010) BART sampler proceeds using backfitting: draws for the k th tree $[(T_k, M_k)|z^*, \{(T_{k'}, M_{k'})\}_{k \neq k'}, \sigma]$ are generated using Chipman et al. (1998) and σ^2 is sampled from an inverse-Gamma distribution. Incorporating these sampling steps into the larger Gibbs sampler in Section 2.3 is straightforward using the `dbarts` package (Dorie et al., 2018).

4 Simulation studies

The proposed STAR modeling framework is evaluated using simulated data, and compared to existing methods for Poisson, negative-binomial, and Gaussian data. Synthetic data y_i for $i = 1, \dots, n$ and $n = 100$ are simulated from the negative-binomial distribution

$$y_i(x) \mid r^*, \lambda_i^* \stackrel{\text{indep}}{\sim} \text{NB} \left\{ r^*, \frac{\lambda_i^*(x)}{r^* + \lambda_i^*(x)} \right\}, \quad x \in \mathcal{X}, \quad (11)$$

where $r^* > 0$ is a dispersion parameter and the negative-binomial distribution is parametrized such that $\mathbb{E}[y_i(x)] = \lambda_i^*(x)$ and $\text{Var}[y_i(x)] = \lambda_i^*(x) \{1 + \lambda_i^*(x)/r^*\}$. As r^* decreases to zero, the variance increasingly dominates the mean while as $r^* \rightarrow \infty$, the distribution converges to a Poisson distribution with parameter $\lambda_i^*(x)$. We select $r^* = 1$ to simulate negative-binomial data with large overdispersion and $r^* = 1000$ to simulate approximate Poisson data. We parametrize the log-mean parameter, $\log \lambda_i^*(x)$, using a linear form (Section 4.1) and a nonlinear form (Section 4.2) to evaluate the STAR models in Sections 3.1 and 3.3, respectively. Additional simulations with log-Gaussian noise are in the Appendix, which produce similar results that strongly favor the STAR models. We emphasize that in all cases, the simulated datasets are *not* generated under the proposed STAR model: they are simulated from negative-binomial and (approximate) Poisson distributions.

Competing models are evaluated and compared using the Watanabe-Akaike/widely-applicable information criteria (WAIC) (Watanabe, 2010). WAIC estimates out-of-sample predictive accuracy using a single model fit requiring only minimal additional computations, and is asymptotically equivalent to cross-validation. The WAIC for a model \mathcal{M} is defined as $\text{WAIC}_{\mathcal{M}} = -2(\text{lppd}_{\mathcal{M}} - d_{\mathcal{M}})$, where $d_{\mathcal{M}}$ is the effective number of parameters for model

\mathcal{M} and $\text{lppd}_{\mathcal{M}}$ is the log-predictive pointwise density defined by

$$\text{lppd}_{\mathcal{M}} = \sum_{i=1}^n \log \left(\frac{1}{S} \sum_{s=1}^S p_{\mathcal{M}}(y_i | \theta^s) \right)$$

for θ^s drawn from its posterior distribution. For STAR with model (3), we simply have

$$\text{lppd}_{\text{STAR}} = \sum_{i=1}^n \log \left(\frac{1}{S} \sum_{s=1}^S \Phi \left\{ \frac{g^s(a_{y_{i+1}}) - \mu^s(x_i)}{\sigma^s(x_i)} \right\} - \Phi \left\{ \frac{g^s(a_{y_i}) - \mu^s(x_i)}{\sigma^s(x_i)} \right\} \right).$$

For the effective number of parameters, we follow the recommendation of Gelman et al. (2014) and use the sample variance of the pointwise log-likelihoods across MCMC simulations: $d_{\mathcal{M}} = \sum_{i=1}^n \text{Var}(\log p(y_i | \theta^s))$. The pointwise (log-) likelihood of STAR is simple and efficient to compute, and is sufficient for computing WAIC as well as other information criteria.

In the Appendix, we also report root mean square errors for estimating the conditional expectation $\lambda_i^*(x)$ in (11), which is useful for comparing point estimation accuracy among competing methods.

4.1 Linear mean functions

We first simulate data from a linear mean function $\mu_i^*(x) = \beta_0 + \sum_{j=1}^p x_{i,j} \beta_j$, where the $p = 6$ predictors are drawn independently from $x_{i,j} \sim N(0, 1)$ and the coefficients are $\beta_0 = \log(1.5)$, $\beta_1 = \beta_2 = \beta_3 = \log(2.0)$, and $\beta_4 = \beta_5 = \beta_6 = 0$. Under this specification, the expected counts at $x_{i,j} = 0$ is 1.5, while each nonzero coefficient β_j for $j = 1, 2, 3$ increases the expected counts by a factor of 2 per one unit change in each x_j .

For comparison, we consider a variety of Bayesian linear regression models. Among STAR models, we use the linear model from Section 3.1 with the ridge prior on β and the following transformations: known transformation (6) with $\lambda = 0$ (LM-STAR-log), $\lambda = 1/2$ (LM-STAR-sqrt), and $\lambda = 1$ (LM-STAR-id); unknown parametric transformation (6) (LM-

STAR-bc); and unknown nonparametric transformation (7) (LM-STAR-np). We also include the same linear model from Section 3.1, but with the Gaussian model (3) applied directly to the raw counts y (LM) and the log-transformed counts $\log(y + 1)$ (LM-log). These models are natural competitors to STAR, since they incorporate the same model for $\mu(x)$ but omit the rounding step in (1) and therefore do not produce an integer-valued distribution. Lastly, we include Poisson (LM-Pois) and negative-binomial (LM-NegBin) linear regression models with a log-link, implemented using the `rstanarm` package (Goodrich et al., 2018). LM-Pois and LM-NegBin are widely used for modeling count data, and under the simulation design (11) correspond to the true data-generating process.

In Figure 2, we plot the relative WAICs across simulated datasets, defined as the ratio between the WAIC of the generic model over the WAIC for a baseline method, for which we select LM-log. Relative WAIC standardizes model performance across simulated datasets: methods with a relative WAIC less than 1.0 demonstrate improvement relative to the baseline method. Notably, the STAR models, particularly LM-STAR-np, LM-STAR-bc, and LM-STAR-log, offer substantial improvements relative to LM-log, and are highly competitive with the true models LM-Pois and LM-NegBin. In particular, the STAR model improvements relative to the Gaussian models LM-log and LM, and the identity transformation LM-STAR-id, definitively demonstrate the importance of the rounding step (1) and the transformation (2), respectively.

4.2 Nonlinear mean functions

To evaluate BART-STAR, we specify a nonlinear form for the log-mean, $\log \lambda_i^*(x) = \beta_0 + \beta_1 \tilde{f}(x)$, where $\tilde{f}(x)$ is the centered and scaled Friedman function (Friedman, 1991)

$$f(x) = 10 \sin(\pi x_1 x_2) + 20(x_3 - 0.5)^2 + 10x_4 + 5x_5 \quad (12)$$

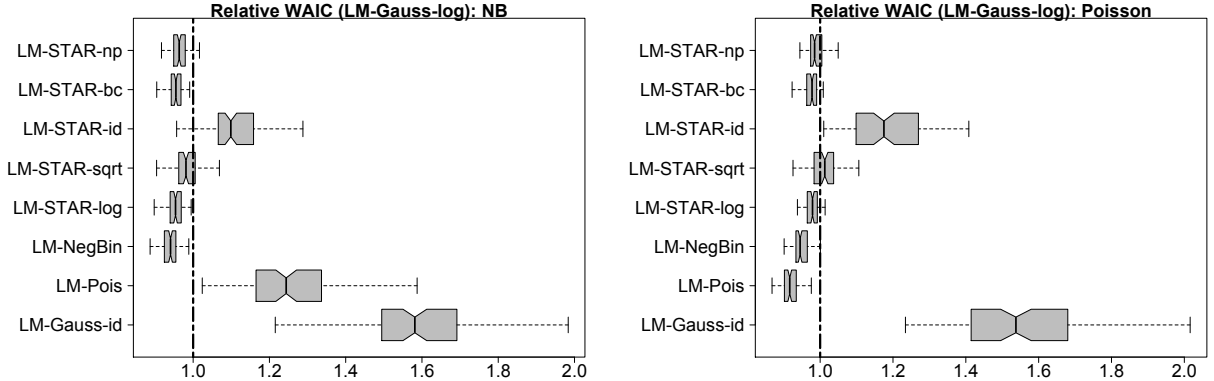


Figure 2: Relative WAIC for negative-binomial (left) and Poisson (right) data with linear mean functions. Preferred models have smaller values, and models with values less than 1.0 are preferred to LM-log. The STAR models outperform the Gaussian models and are highly competitive with the true models LM-Pois and LM-NegBin.

featured in the original BART simulations (Chipman et al., 2010). As in Chipman et al. (2010), we select $p = 10$ and simulate $x_{i,j} \stackrel{iid}{\sim} \text{Uniform}(0, 1)$. We fix the parameters $\beta_0 = \log(1.5)$ and $\beta_1 = \log(5.0)$, which again corresponds to low counts with a moderate signal.

We combine the BART-STAR model of Section 3.3 with known transformation (6) for $\lambda = 0$ (BART-STAR-log), $\lambda = 1/2$ (BART-STAR-sqrt), and $\lambda = 1$ (BART-STAR-id); unknown parametric transformation (6) (BART-STAR-bc); and unknown nonparametric transformation (7) (BART-STAR-np). For competitors, we include the Gaussian BART model (BART-id) of Chipman et al. (2010) and a Gaussian BART model on the log-transformed counts $\log(y + 1)$ (BART-log). Lastly, we include the linear models LM-STAR-bc and LM-log from Section 4.1.

The relative WAICs are plotted in Figure 3, where again we use the log-transformed Gaussian model (BART-log) as the baseline. Both BART-STAR-id and BART-id are omitted as noncompetitive. BART-STAR provides substantial improvements relative to BART and linear Gaussian models, with especially strong performance from BART-STAR-np, BART-STAR-bc, and BART-STAR-log. Perhaps surprisingly, the STAR linear model LM-STAR-bc outperforms both the plain BART-id and BART-log for negative-binomial data, despite the nonlinearity in (12). By comparison, BART-STAR-bc consistently outperforms LM-STAR-bc, which suggests

that the proposed BART-STAR model is capable of detecting the nonlinear features in (12).

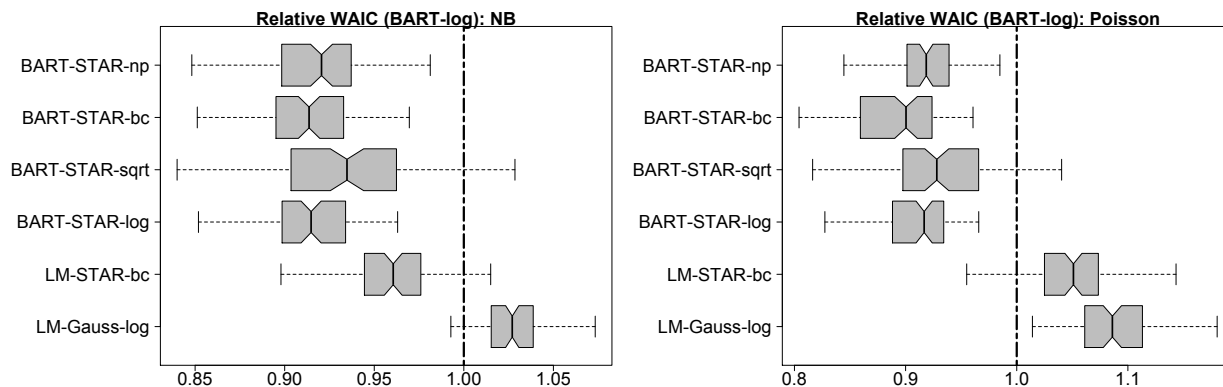


Figure 3: Relative WAIC for negative-binomial (left) and Poisson (right) data with nonlinear mean functions. Preferred models have smaller values, and models with values less than 1.0 are preferred to BART-log. The identity models (BART-id, BART-STAR-id) are omitted since they are noncompetitive, with relative WAICs above 1.6. The BART-STAR models are clearly superior.

5 Illustrations

We apply the proposed STAR models of Section 3 to a variety of applications. We focus on two applications in particular, the demand for medical care (Section 5.1) and the population of tucuxi dolphins in the Amazon River (Section 5.2). In the Appendix, we provide WAIC comparisons for several additional datasets, with the same general conclusions: (i) both the rounding and the transformation in STAR substantially improve model performance and (ii) the nonlinear (additive and BART) STAR models are typically preferred.

5.1 National Medical Expenditure Survey data

To study the demand for medical care, Deb and Trivedi (1997) analyze data from the National Medical Expenditure Survey (NMES) conducted in 1987 and 1988, which is available in the AER package in R (Kleiber and Zeileis, 2008). Deb and Trivedi (1997) and Cameron and Trivedi (2013) consider $n = 4406$ elderly adults (aged 66 and older) covered by Medicare,

with a variety of health measures, socioeconomic and demographic variables, and indicators of each patient’s type of insurance. Multiple response measures of healthcare utilization are available, including physician office visits (`visits`), non-physician office visits (`nvisits`), physician hospital outpatient visits (`ovisits`), and non-physician hospital outpatient visits (`novisits`). Each response is integer-valued with distinct characteristics: the probability mass functions in Figure 4 illustrate the differences in the marginal distributions, most notably the proportion of zeros and the degree of overdispersion. Broadly, it is important to know which patient characteristics correspond to healthcare utilization, as well as to predict which patients will seek medical care, and how frequently.

The NMES data provides the opportunity for insightful model comparisons. Using the same set of $n = 4406$ individuals and $p = 17$ predictors, we compare model performance among the linear, additive, and BART regression models using each of the four response variables `visits`, `nvisits`, `ovisits`, and `novisits`. The WAIC comparisons are in Table 1. In general, the STAR-log, STAR-bc, and STAR-np models dominate, usually with BART-STAR outperforming the linear and additive models. Interestingly, the STAR linear model is preferred for `novisits`, which has the greatest zero-inflation and overdispersion. Despite the distributional differences among the measures of healthcare demand, STAR provides the best linear, additive, and BART model fits in all four cases.

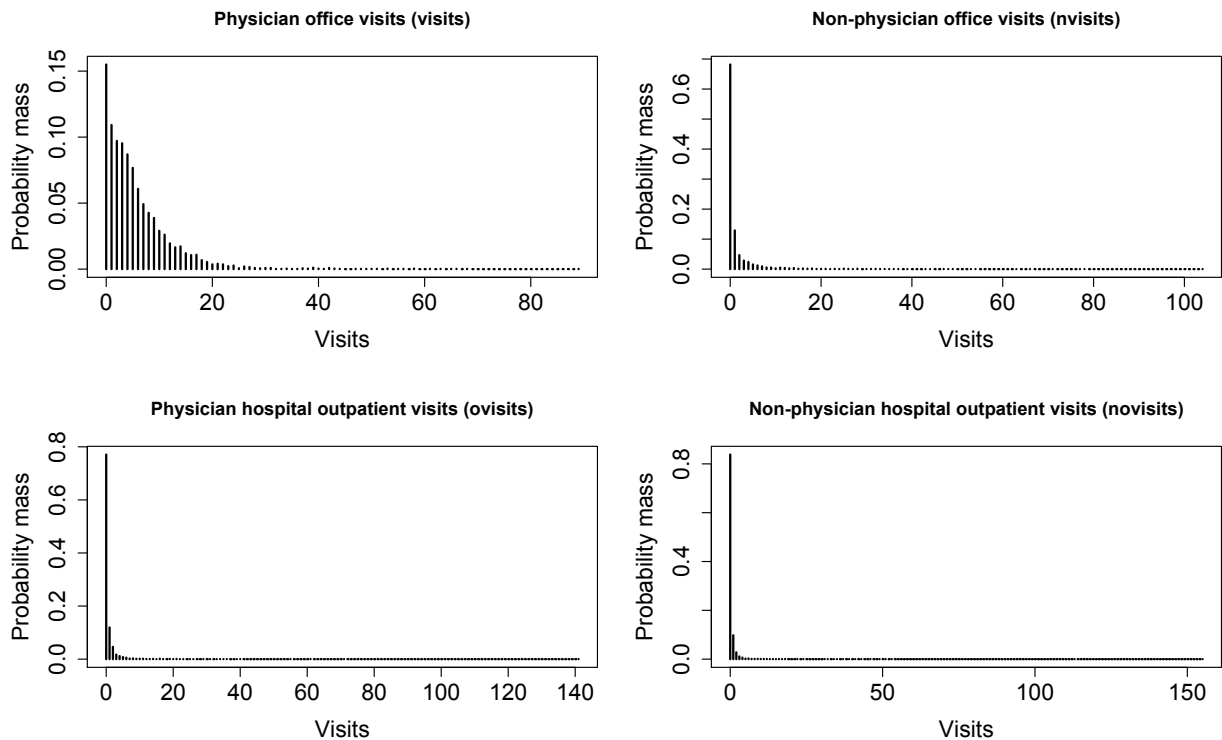


Figure 4: Probability mass functions for each measure of medical care demand. Zero-inflation and overdispersion are present in each case to varying degrees.

		Gauss-id	Gauss-log	STAR-log	STAR-bc	STAR-np	Pois	NB
visits	LM	28906	24446	24629	24290	24225	36416	24446
	AM	28900	24433	24618	24278	24294	-	-
	BART	28918	24375	24554	24233	24170	-	-
nvisits	LM	27208	14055	11743	11741	11815	29122	11912
	AM	27208	14060	11744	11744	11798	-	-
	BART	27005	14061	11741	11743	11782	-	-
ovisits	LM	24302	9577	8134	8136	8138	16247	8244
	AM	24264	9585	8135	8136	8171	-	-
	BART	29160	9572	8116	8115	8138	-	-
novisits	LM	25015	7280	6029	6030	6003	14753	6280
	AM	25031	7291	6033	6035	6013	-	-
	BART	24369	7287	6044	6045	6015	-	-

Table 1: WAIC for the NMES data for each response. The best method (lowest WAIC) for each linear model (LM), additive model (AM), and BART model is in bold, and the best overall model for each response is underlined. STAR provides the best linear, additive, and BART model fits in all four cases.

For further model evaluation, we compute posterior predictive diagnostics for the `nvisits` data under BART-log, BART-STAR-id, and BART-STAR-bc. The posterior predictive draws were simulated as in Section 2.3, and evaluated using the sample mean, the sample standard deviation, and the proportion of zeros, which cumulatively address the ability of each model to capture overdispersion and zero-inflation. Since BART-log models $\log(y + 1)$ as conditionally Gaussian, the posterior predictive draws in that case were generated by simulating Gaussian BART posterior predictive draws, say \tilde{y} , and computing $\exp(\tilde{y}) - 1$. The results are plotted in Figure 5. Clearly, both rounding *and* transformation are essential to produce an adequate model: the unrounded model BART-log and the untransformed model BART-STAR-id are decisively inadequate for the data. This model misspecification is *not* simply due to an overly restrictive model for the regression effects: each model uses an identical BART parametrization for $\mu(x)$, which is known to offer substantial flexibility.

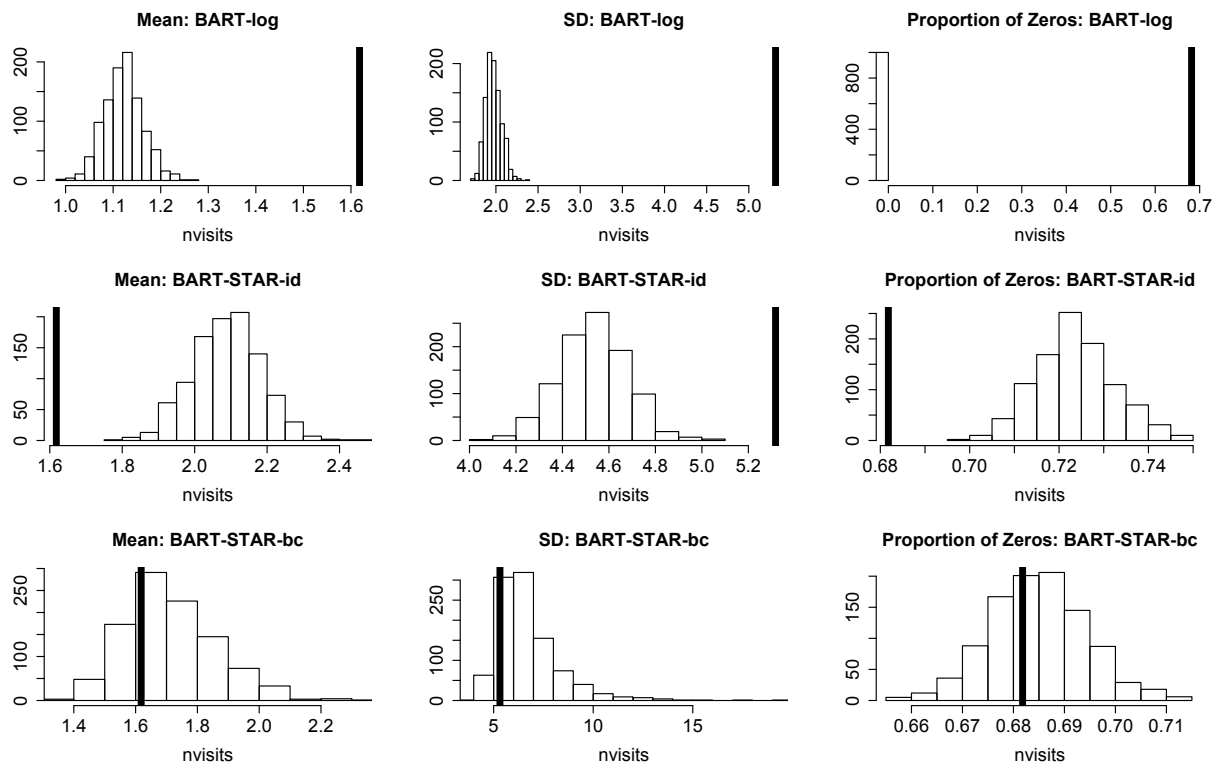


Figure 5: Posterior predictive diagnostics for BART-log (top row), BART-STAR-id (middle row), and BART-STAR-bc (bottom row). The mean (left), standard deviation (center), and proportion of zeros (right) were computed for each posterior predictive simulated dataset (histograms) and the observed data y (vertical lines). Only the model including both transformation *and* rounding (BART-STAR-bc) is adequate for the `nvisits` data.

In Figure 6, we compare posterior inference on the linear regression coefficients between LM-STAR-log and LM-NegBin for the response variable `visits`. Despite the distinct distributional assumptions, inference for the coefficients is remarkably similar. Strong positive effects on the number of physician office visits include both insurance indicators, private insurance (`insuranceyes`) and Medicaid (`medicaidyes`), self-perceived poor health (`healthpoor`), the number of chronic health conditions (`chronic`), living in the western United States (`regionwest`), and the number of years in school (`school`), while strong negative effects are self-perceived excellent health (`healthexcellent`), gender (`gendermale`), and African American ethnicity (`afamyces`). MCMC diagnostics for β_j and σ reported in the Appendix

demonstrate exceptional MCMC mixing with no lack of convergence.

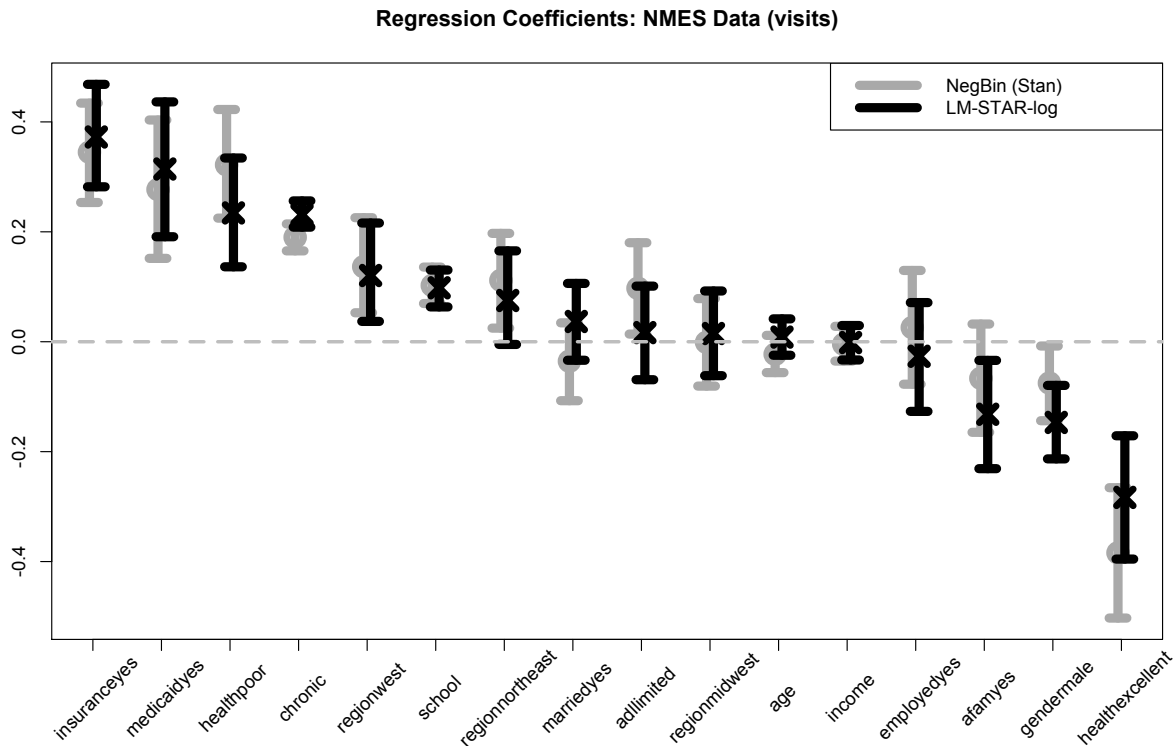


Figure 6: Posterior expectation and 95% credible intervals for the regression coefficients β_j under LM-NegBin (gray) and LM-STAR-log (black) for the `visits` data.

5.2 Amazon river dolphins data

The tucuxi dolphin (*sotalia fluviatilis*) is a small river dolphin that inhabits the Amazon River. While the tucuxi dolphin population was once stable, the progression of habitat degradation, dolphin fishing, and other human interference has to led to increased concerns of population decline. To assess the validity of these concerns, da Silva et al. (2018) recently analyzed data collected from 1994 to 2017 in which multiple observers searched for tucuxi dolphins along a particular segment of the Amazon River. In addition to the number of tucuxi dolphins observed, data report the water level (in meters), the number of observers present,

and the date for each of $n = 312$ surveys. While da Silva et al. (2018) fit a linear model to the logarithm of dolphin counts, we propose to leverage the STAR modeling framework to investigate nonlinear effects and provide greater distributional flexibility.

We apply additive STAR models to study the yearly evolution of tucuxi dolphin counts, which may be nonlinear, while adjusting for seasonal, water level, and observer effects. Specifically, for each survey we include the year (`year`), day-of-year (`doy`), and water level (`water`) as nonlinear predictors and the number of observers (`obs`) as a linear predictor. For completeness, we consider all linear, additive, and BART models from Section 5.1, and report the WAICs in the Appendix. Again, the STAR models dominate, and the nonparametric transformation (STAR-np) provides the best linear, additive, and BART models.

For the additive STAR-np model, we plot posterior expectations and credible intervals for each f_j in Figure 7. The `doy` plot suggests a seasonal pattern, while the `water` plot exhibits an approximately quadratic effect. Most importantly, the `year` plot shows a near linear decline in tuxucis dolphins from 1994-2017, which interestingly has leveled off since 2013. These findings are partially consistent with the results of da Silva et al. (2018) which, assuming only a linear model, also report a significant decrement of dolphins since 1994. Posterior predictive diagnostics demonstrate the adequacy of the STAR approach, especially compared to untransformed and unrounded models, and MCMC diagnostics for f_j show exceptional MCMC mixing with no lack of convergence (see the Appendix).

6 Discussion

STAR processes provide a modeling framework for adapting state-of-the-art models for continuous data to produce coherent models for integer-valued data. STAR offers remarkable modularity by building upon both continuous data models and the accompanying algorithms for estimation, which we leverage to develop new linear regression models, additive models, and

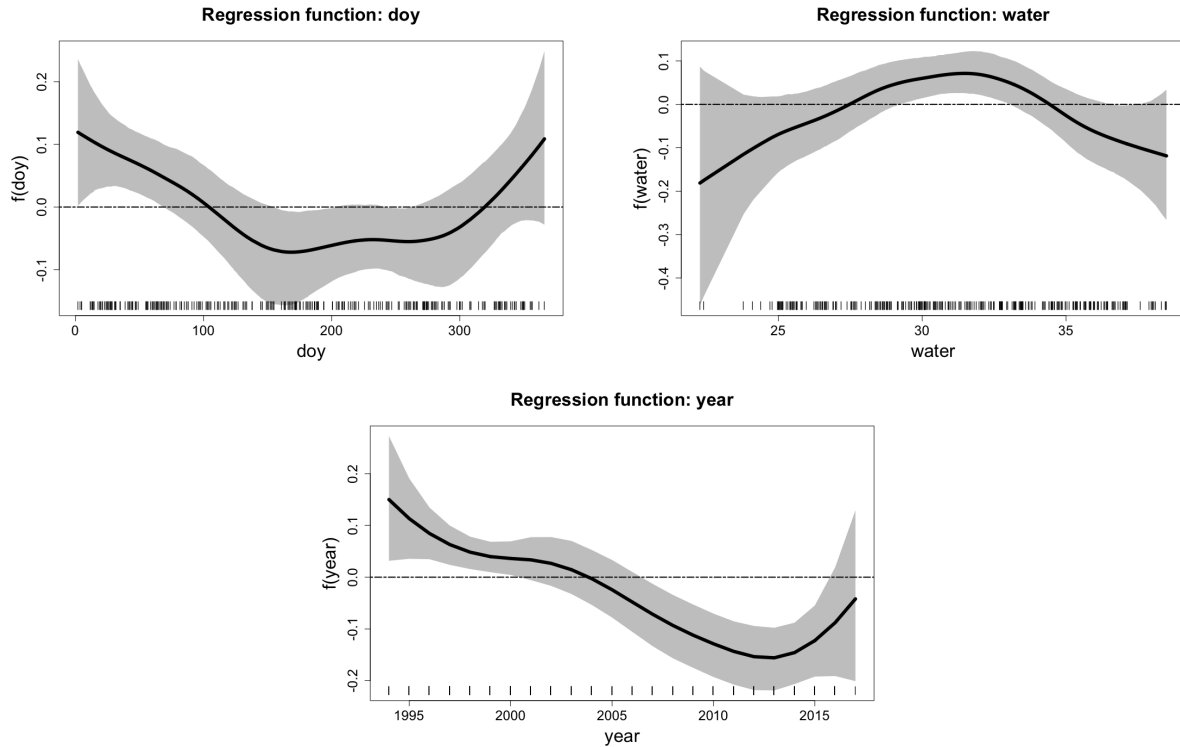


Figure 7: Posterior expectation and 95% pointwise credible intervals for the regression smoothing functions $f_j(v_j)$ under the additive STAR-np model for the tucuxis dolphin data. The tick marks indicate the observation points for each predictor.

BART for integer-valued data. By incorporating known, unknown parametric, and unknown nonparametric transformations, we provide varying degrees of distributional flexibility, and show that STAR processes can model important distributional features such as zero-inflation, bounded or censored data, and over- or underdispersion. Through simulation studies and several real data applications, we demonstrate the exceptional performance of STAR relative to existing Gaussian and count data models, and validate STAR model adequacy and STAR MCMC efficiency for two applications of interest.

A variety of promising extensions exist for STAR. The modeling and computational modularity of STAR suggest that new multivariate, functional, and time series models may be developed for integer-valued data. Furthermore, STAR is capable of modeling rounded data,

which is ubiquitous in practice yet rarely considered in modern statistical and machine learning methods. Lastly, the STAR model (1)-(2) does not strictly require a Bayesian modeling approach, and may be adapted for classical estimation and inference.

S Supplementary Material

S.1 Additional simulation results

To supplement the simulation study from Section 4, we modify the log-mean $\lambda_i^*(x)$ to include log-Gaussian noise:

$$\log \lambda_i^*(x) = \mu_i^*(x) + \sigma^* \epsilon_i^*, \quad \epsilon_i^* \stackrel{iid}{\sim} N(0, 1) \quad (\text{S.1})$$

We let $\sigma^* = \sqrt{2 \log(1.5)} \approx 0.90$, which implies that $\mathbb{E}[\lambda_i^*(x)] = 1.5 \exp(\mu_i^*(x))$ is inflated by 50%. We parametrize the log-mean parameter, $\mu_i^*(x)$, using a linear form (Section 4.1) and a nonlinear form (Section 4.2) to evaluate the STAR models in Sections 3.1 and 3.3, respectively. The results for negative-binomial ($r^* = 1$) and approximate Poisson ($r^* = 1000$) data with log-normal innovations are displayed in Figures S.1 and S.2 for the linear and nonlinear mean functions, respectively. The results are consistent with those in the main paper, namely that STAR outperforms the Gaussian methods and is highly competitive with LM-NegBin. For the linear models in Figures S.1, the STAR models now also outperform LM-Pois by a wide margin.

To accompany the WAIC comparisons from Section 4, we evaluate each method for point estimation accuracy. Specifically, we are interested in estimating the conditional expectation of the observed data, $\lambda_i^*(x)$. For an estimator $\hat{y}_i(x)$, we compute the root mean squared error $\text{RMSE} = \sqrt{\sum_{i=1}^n \{\lambda_i^*(x) - \hat{y}_i(x)\}^2}$. The fitted values for STAR are computed using the

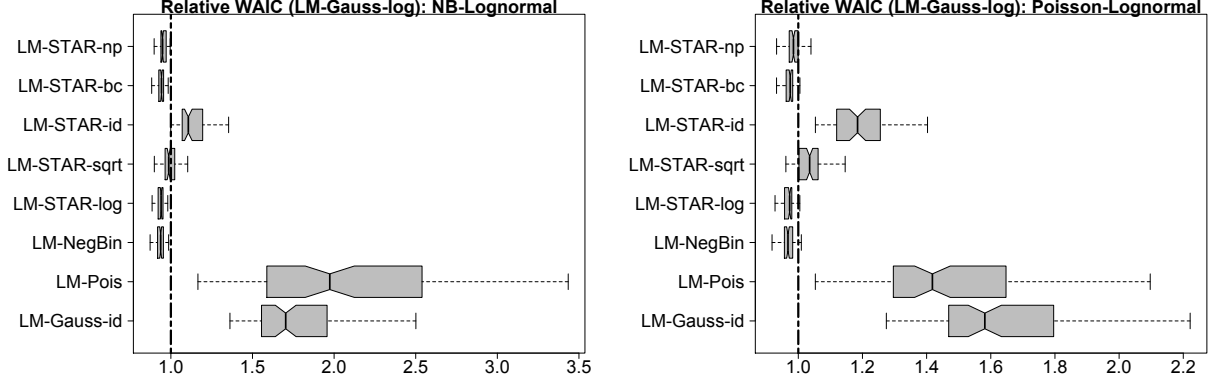


Figure S.1: Relative WAIC for negative-binomial (left) and Poisson (right) data with log-Gaussian innovations and linear mean functions. Preferred models have smaller values, and models with values less than 1.0 are preferred to LM-log. The STAR models clearly outperform the Gaussian models and LM-Pois, and perform similarly to LM-NegBin.

conditional expectation of y at $x \in \mathcal{X}$, that is

$$\mathbb{E}\{y(x)\} = \sum_{j=0}^{\infty} j\mathbb{P}\{y(x) = j\} \approx \sum_{j=1}^{J(x)} j\mathbb{P}\{y(x) = j\}, \quad (\text{S.2})$$

where $\mathbb{P}\{y(x) = j\}$ is the STAR probability mass function and $J(x)$ is a finite truncation. Since $\mathbb{P}\{y(x) = j\}$ depend on the parameters θ in Π_{θ} , the posterior distribution of (S.2) may be computed by evaluating (S.2) for each draw of θ in the MCMC algorithm. Conservatively, we select $J(x)$ to be the 99.99th quantile of the distribution of $y(x)$ pointwise for each x , which is easily computable as $h[g^{-1}\{z_q^*(x)\}]$ where $z_q^*(x)$ is the q th quantile of Π_{θ} . The point estimate is computed as the posterior expectation of (S.2).

Figures S.3 and S.4 depict the relative RMSEs across simulated data sets for the linear and nonlinear simulation designs in Sections 4.1 and 4.2, respectively, defined as the ratio between the RMSE of the generic model over the RMSE for a baseline method, and specifically the LM-log method which represents the common approach of modeling (log-) transformed counts using Gaussian models. Relative RMSE standardizes model performance across simulated datasets: methods with a relative RMSE less than 1.0 demonstrate superior

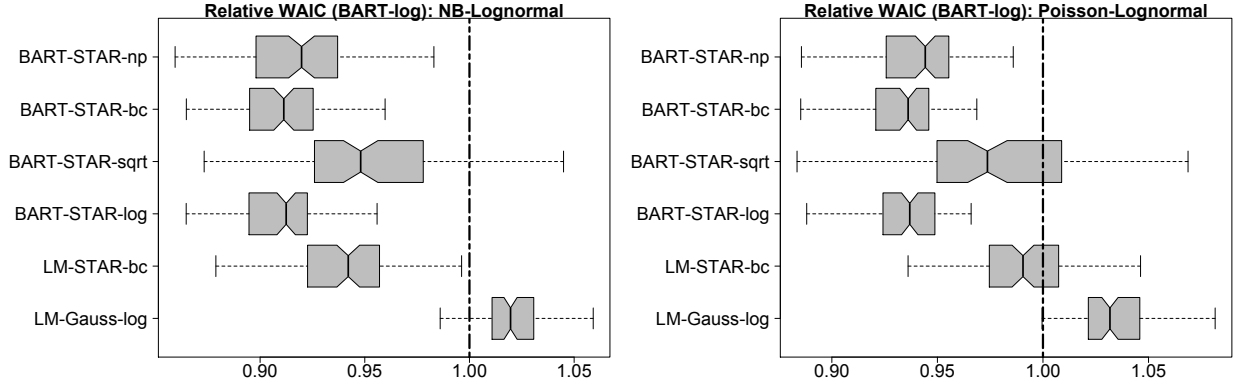


Figure S.2: Relative WAIC for negative-binomial (left) and Poisson (right) data with log-Gaussian innovations and nonlinear mean functions. Preferred models have smaller values, and models with values less than 1.0 are preferred to BART-log. The identity models (BART-id, BART-STAR-id) are omitted since they are noncompetitive. The BART-STAR models are clearly superior.

point estimation relative to the baseline method. As in Section 4, we find that STAR-log and STAR-bc are consistently competitive and outperform other methods. Interestingly, STAR-np is much less competitive in RMSE than in WAIC, which suggests that the additional distributional flexibility acquired by modeling g nonparametrically does not necessarily imply more accurate point estimation.

S.2 Additional results on NMES data

To validate the inference in Figure 6 for the LM-STAR-log model applied to the `visits` data, we include traceplots for the regression coefficients β_j and the error standard deviation σ in Figure S.5. Posterior inference was conducted based on an MCMC chain of 1000 iterations (after discarding a burn-in of 1000 and retaining every 3rd sample). The traceplots indicate no lack of convergence and demonstrate exceptional mixing: effective sample sizes for all coefficients β_j and σ exceeded 900.

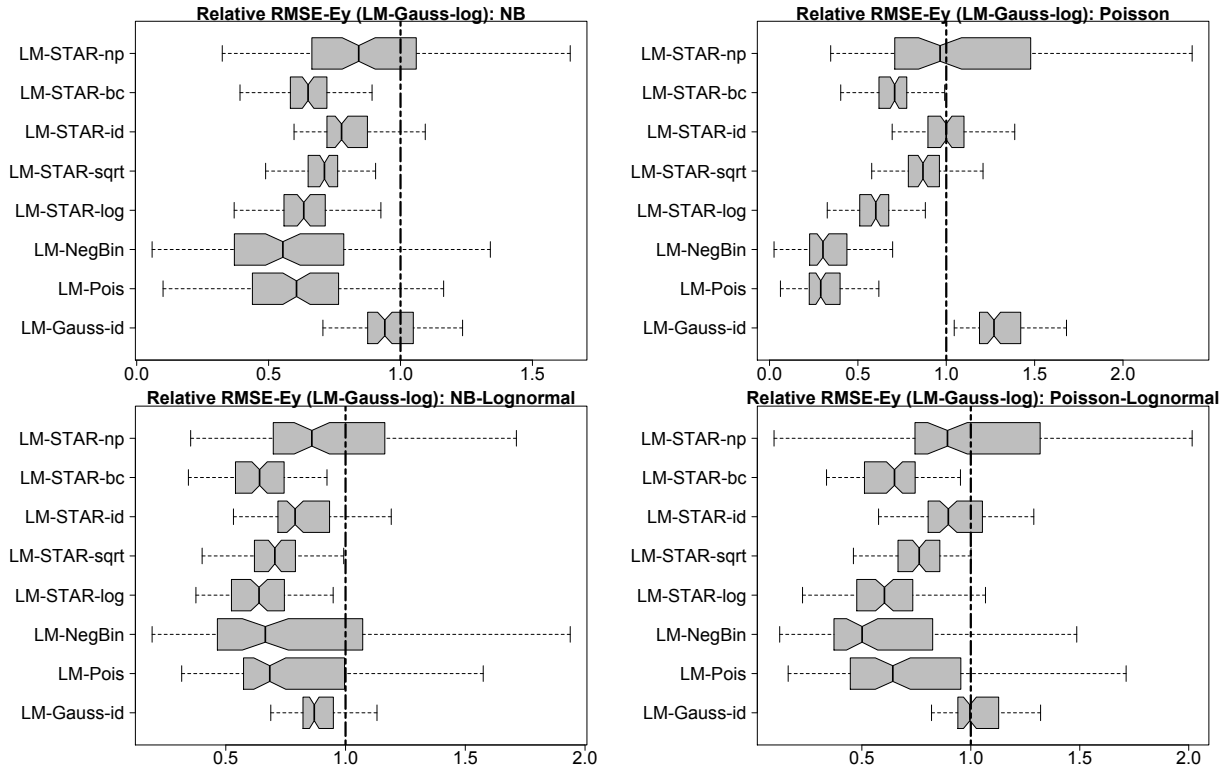


Figure S.3: Relative RMSE under various distributions. Preferred models have smaller values, and models with values less than 1.0 are preferred to LM-log. As expected, the LM-NegBin performs well, since it closely matches the data-generating process. Notably, the STAR models are highly competitive, and clearly superior to the Gaussian models, especially LM-STAR-bc and LM-STAR-log.

S.3 Additional results on Amazon river dolphins data

In Table S.1, we report the WAICs for the tucuxis dolphins data. The STAR model with nonparametric transformation (STAR-np) provides the best linear, additive, and BART model for these data.

Posterior predictive diagnostics for additive models fit to the tucuxis dolphins data are in Figure S.6. Notably, the additive STAR-np model is adequate for the data, while the models which lack either rounding or transformation are incapable of capturing distributional features, including the variability and the proportion of zeros. The MCMC convergence of the additive STAR-np model is assessed via traceplots in Figure S.7. The traceplots indicate

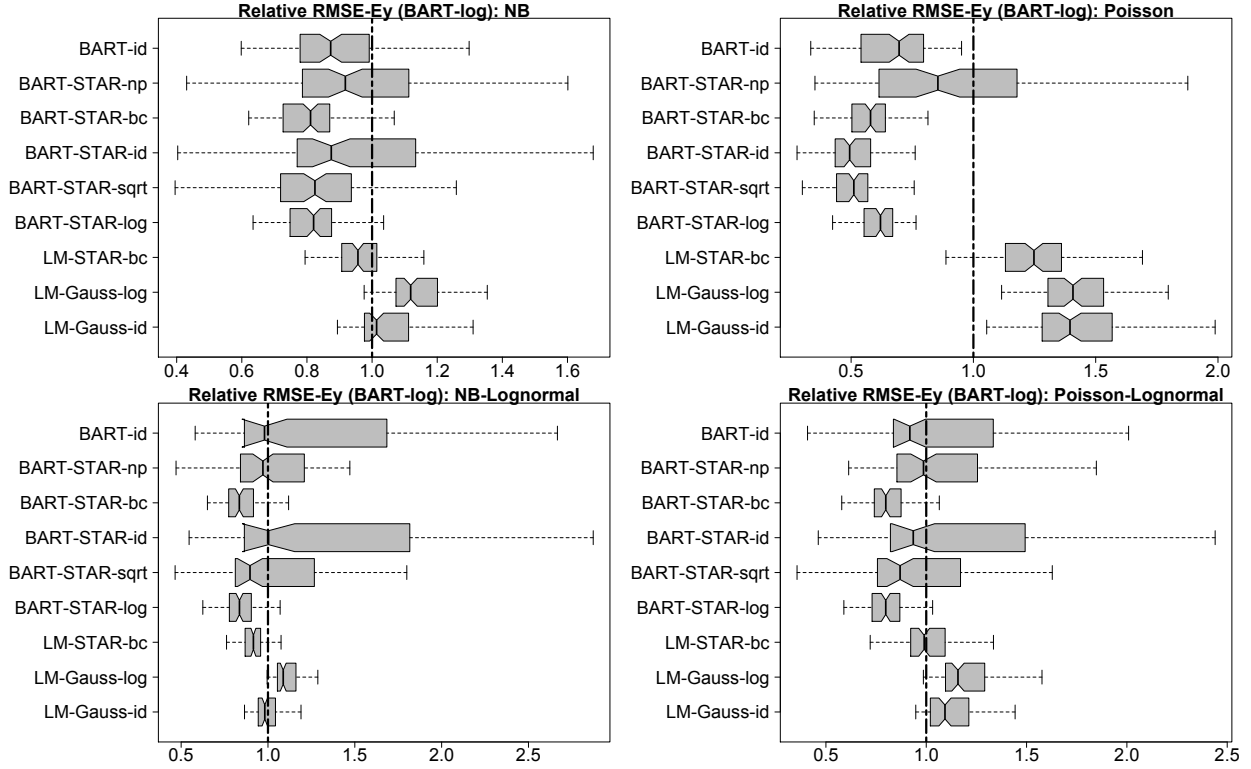


Figure S.4: Relative RMSE under various distributions. Preferred models have smaller values, and models with values less than 1.0 are preferred to BART-log.

no lack of convergence and demonstrate exceptional mixing: effective sample sizes for all $f_j(v_j)$ exceed 2000.

S.4 Additional Empirical Illustrations

For further models comparisons, we apply the linear, additive, and BART models from Section 5.1 to several additional datasets, and again consider STAR, Gaussian, Poisson, and negative-binomial distributions. For all additive models, we partition $x = (u, v)$ in (9) such that v contains all continuous variables (with at least 10 unique observation points), which are therefore modeled nonlinearly.

Traceplots: Regression Coefficients

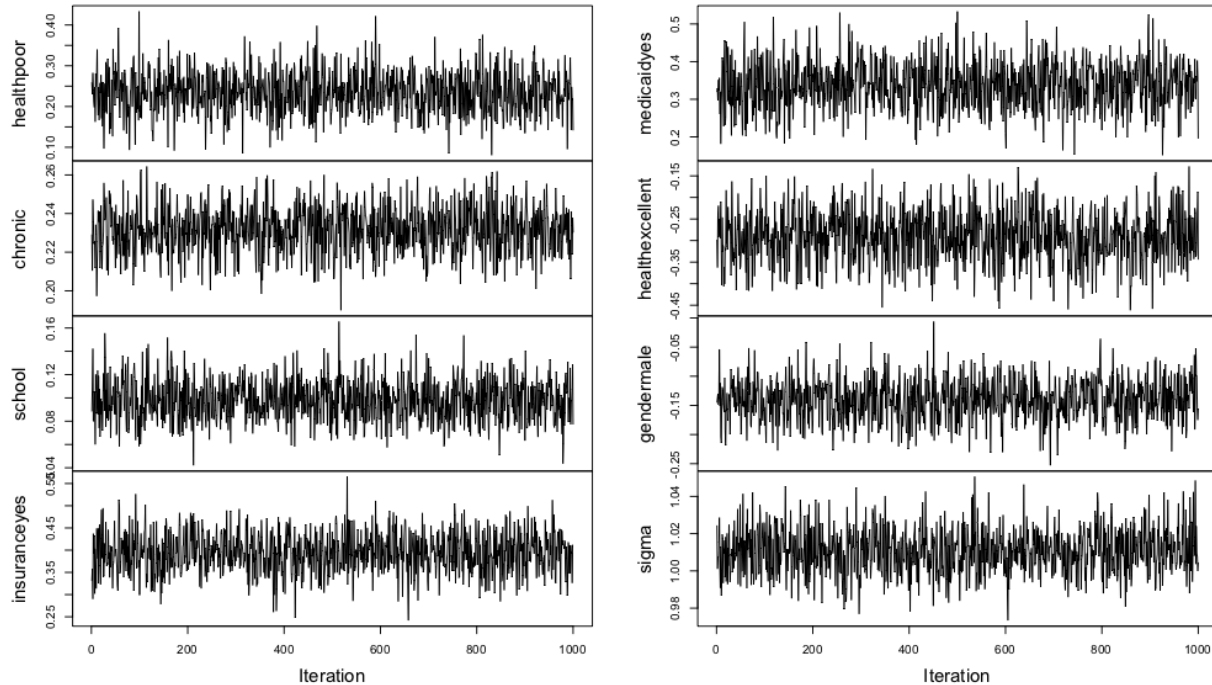


Figure S.5: Traceplots for β_j and σ under LM-STAR-log for the NMES visits data. Posterior inference in Figure 6 was conducted based on an MCMC chain of 1000 iterations (after discarding a burn-in of 1000 and retaining every 3rd sample). Effective sample sizes for all coefficients β_j and σ exceeded 900.

S.4.1 Ships Data

The ships data, available in the MASS package in R, provides the number of damage incidents due to waves for $n = 34$ cargo-carrying vessels, as well as ship type (A-E), year of construction (1960-1964, 1965-1969, 1970-1974, or 1975-1979), the period of construction (1960-1974 or 1975-1979), and the aggregated months of service (ranging from 0 to 44882). We model the ship type, year of construction, and period of construction as factors, and center and scale the service variable. The data were analyzed in McCullagh and Nelder (1989) using a quasi-Poisson regression model to account for observed overdispersion, and subsequently re-analyzed in Mallick and Gelfand (1994) using a Poisson regression model with unknown

	Gauss-id	Gauss-log	STAR-log	STAR-sqrt	STAR-id	STAR-bc	STAR-np	Pois	NB
Linear	2190	2009	2033	1960	2025	1961	1956	3096	1966
Additive	2172	1965	1990	1924	2001	1925	1918	-	-
BART	2146	1941	1956	1888	1966	1889	<u>1886</u>	-	-

Table S.1: WAIC for the tucuxis dolphin data. The best method (lowest WAIC) for each model class is in bold, and the best overall model is underlined. STAR-np provides the best linear, additive, and BART model fits.

link function, which suggests that additional distributional flexibility in the regression model may be important.

S.4.2 Roaches Data

Gelman and Hill (2006) consider a study of pest management for eliminating cockroaches in city apartments. The response variable, y_i , is the number of roaches caught in traps in apartment i , with $i = 1, \dots, n = 262$. A pest management treatment was applied to a subset of 158 apartments, with the remaining 104 apartments receiving a control. Additional data are available on the pre-treatment number of roaches, whether the apartment building is restricted to elderly residents, and the number of days for which the traps were exposed. A notable feature of the data is zero-inflation: $y_i = 0$ for 94 (36%) of the apartments.

S.4.3 Highway Data

The Highway data, available in the `carData` package in R, consists of the 1973 accident rate per million vehicle miles on $n = 39$ large sections of Minnesota highway. Important predictors include the number of access points per mile, the speed limit, the width of the outer shoulder on the roadway (in feet), and the number of signals per mile of roadway, among others. We consider the accident rate per 10,000 miles, which is the smallest rate for which the observations y_i are integer-valued. A notable feature of these data are that, despite being (scaled) accident counts, no two observations y_i and y_j are equal, and the counts themselves are large, ranging from 161 to 923. Therefore, it is unclear *a priori* whether an

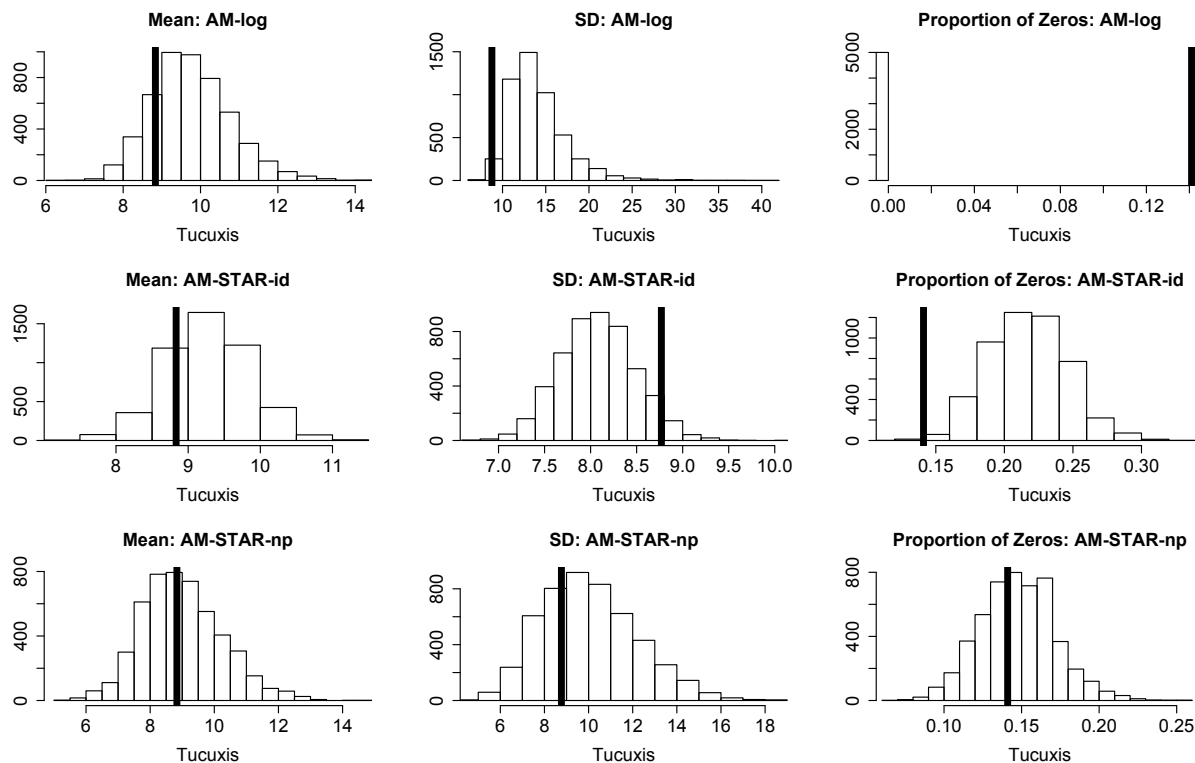


Figure S.6: Posterior predictive diagnostics for AM-log (top row), AM-STAR-id (middle row), and AM-STAR-np (bottom row). The mean (left), standard deviation (center), and proportion of zeros (right) were computed for each posterior predictive simulated dataset (histograms) and the observed data y (vertical lines). Only the model including both transformation *and* rounding (AM-STAR-np) is adequate for the dolphin data.

integer-valued model is necessary or advantageous.

S.4.4 Results

The WAICs for the supplementary datasets are reported in Table S.2. The STAR models consistently perform well across all datasets, and in particular STAR-bc and STAR-np. Notably, STAR provides the best linear, additive, and BART models for all datasets with the exception of the Highway data, for which all BART models perform similarly. Interestingly, additive STAR models are preferred for both the `ships` data and the Highway data, while BART-STAR is slightly preferred to the additive STAR model for the `roaches` data.

Traceplots: Additive Model Parameters

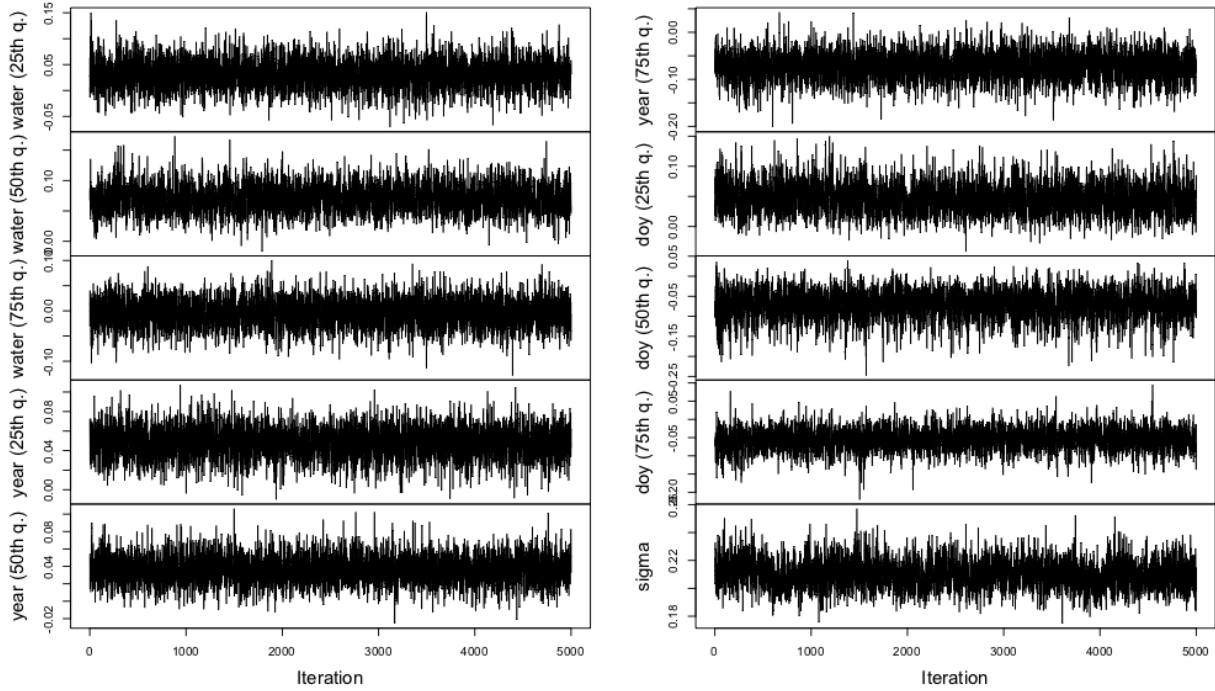


Figure S.7: Traceplots for $f_j(v_j)$ and σ under the additive STAR-np model for the dolphin data, where the functions f_j are evaluated at the 25th, 50th, and 75th sample quantiles of each $\{v_{i,j}\}_{i=1}^n$. Posterior inference in Figure 7 was conducted based on an MCMC chain of 5000 iterations (after discarding a burn-in of 5000 and retaining every 3rd sample). Effective sample sizes for all $f_j(v_j)$ exceeded 2000.

	Model	Gauss-id	Gauss-log	STAR-log	STAR-sqrt	STAR-id	STAR-bc	STAR-np	Pois	NB
ships	LM	292	204	204	195	220	196	194	239	203
	AM	240	188	193	173	182	175	<u>171</u>	-	-
	BART	242	204	200	182	191	196	187	-	-
roaches	LM	2722	1886	1791	1772	1952	1756	1759	12565	1793
	AM	2711	1838	1740	1732	1928	1710	1729	-	-
	BART	2700	1833	1736	1732	1927	<u>1708</u>	1719	-	-
Highway	LM	495	481	481	484	496	486	479	1587	496
	AM	487	465	465	473	484	478	460	-	-
	BART	466	463	465	465	469	476	464	-	-

Table S.2: WAIC for the **ships**, **roaches**, and **Highway** datasets. The best method (lowest WAIC) for each model class is in bold, and the best overall model for each outcome is underlined. The STAR models dominate, with the additive and BART models typically outperforming the linear models.

References

- Bai, J., Sun, Y., Schrack, J. A., Crainiceanu, C. M., and Wang, M.-C. (2018). A two-stage model for wearable device data. *Biometrics*, 74(2):744–752.
- Bening, V. E. and Korolev, V. Y. (2012). *Generalized Poisson models and their applications in insurance and finance*. Walter de Gruyter.
- Bhattacharya, A., Chakraborty, A., and Mallick, B. K. (2016). Fast sampling with gaussian scale mixture priors in high-dimensional regression. *Biometrika*, 103(4):985–991.
- Box, G. E. and Cox, D. R. (1964). An analysis of transformations. *Journal of the Royal Statistical Society: Series B (Methodological)*, 26(2):211–243.
- Cameron, A. C. and Trivedi, P. K. (2013). *Regression analysis of count data*, volume 53. Cambridge university press.
- Canale, A. and Dunson, D. B. (2011). Bayesian kernel mixtures for counts. *Journal of the American Statistical Association*, 106(496):1528–1539.
- Canale, A. and Dunson, D. B. (2013). Nonparametric Bayes modelling of count processes. *Biometrika*, 100(4):801–816.
- Carota, C. and Parmigiani, G. (2002). Semiparametric regression for count data. *Biometrika*, 89(2):265–281.
- Carvalho, C. M., Polson, N. G., and Scott, J. G. (2010). The horseshoe estimator for sparse signals. *Biometrika*, pages 465–480.
- Chipman, H. A., George, E. I., and McCulloch, R. E. (1998). Bayesian CART model search. *Journal of the American Statistical Association*, 93(443):935–948.

- Chipman, H. A., George, E. I., and McCulloch, R. E. (2010). BART: Bayesian additive regression trees. *The Annals of Applied Statistics*, 4(1):266–298.
- Crainiceanu, C., Ruppert, D., and Wand, M. P. (2005). Bayesian analysis for penalized spline regression using WinBUGS. *Journal of Statistical Software*, 14(14):1–24.
- da Silva, V. M., Freitas, C. E., Dias, R. L., and Martin, A. R. (2018). Both cetaceans in the Brazilian Amazon show sustained, profound population declines over two decades. *PloS one*, 13(5):e0191304.
- Deb, P. and Trivedi, P. K. (1997). Demand for medical care by the elderly: a finite mixture approach. *Journal of Applied Econometrics*, 12(3):313–336.
- Dorazio, R. M., Jelks, H. L., and Jordan, F. (2005). Improving removal-based estimates of abundance by sampling a population of spatially distinct subpopulations. *Biometrics*, 61(4):1093–1101.
- Dorie, V., Chipman, H., and R, M. (2018). *dbarts: Discrete Bayesian Additive Regression Trees Sampler*. R package version 3.1.
- Duan, L. L., Johndrow, J. E., and Dunson, D. B. (2018). Scaling up data augmentation MCMC via calibration. *The Journal of Machine Learning Research*, 19(1):2575–2608.
- Famoye, F. (1993). Restricted generalized Poisson regression model. *Communications in Statistics-Theory and Methods*, 22(5):1335–1354.
- Ferguson, T. S. (1973). A bayesian analysis of some nonparametric problems. *The annals of statistics*, pages 209–230.
- Friedman, J. H. (1991). Multivariate adaptive regression splines. *The annals of statistics*, pages 1–67.

- Gelman, A. and Hill, J. (2006). *Data analysis using regression and multilevel/hierarchical models*. Cambridge university press.
- Gelman, A., Hwang, J., and Vehtari, A. (2014). Understanding predictive information criteria for Bayesian models. *Statistics and computing*, 24(6):997–1016.
- Goodrich, B., Gabry, J., Ali, I., and Brilleman, S. (2018). rstanarm: Bayesian applied regression modeling via Stan. R package version 2.17.4.
- Hilbe, J. M. (2011). *Negative binomial regression*. Cambridge University Press.
- Klami, A. (2015). Pólya–Gamma augmentations for factor models. In *Asian Conference on Machine Learning*, pages 112–128.
- Kleiber, C. and Zeileis, A. (2008). *Applied Econometrics with R*. Springer-Verlag, New York. ISBN 978-0-387-77316-2.
- Kowal, D. R. (2019). Integer-valued functional data analysis for measles forecasting. *Biometrics*. Forthcoming.
- Linero, A. R. (2018). Bayesian regression trees for high-dimensional prediction and variable selection. *Journal of the American Statistical Association*, 113(522):626–636.
- Linero, A. R. and Yang, Y. (2018). Bayesian regression tree ensembles that adapt to smoothness and sparsity. *Journal of the Royal Statistical Society: Series B (Statistical Methodology)*, 80(5):1087–1110.
- Lord, D., Guikema, S. D., and Geedipally, S. R. (2008). Application of the Conway–Maxwell–Poisson generalized linear model for analyzing motor vehicle crashes. *Accident Analysis & Prevention*, 40(3):1123–1134.

- Mallick, B. K. and Gelfand, A. E. (1994). Generalized linear models with unknown link functions. *Biometrika*, 81(2):237–245.
- Matteson, D. S., McLean, M. W., Woodard, D. B., and Henderson, S. G. (2011). Forecasting emergency medical service call arrival rates. *The Annals of Applied Statistics*, 5(2B):1379–1406.
- McCullagh, P. (1980). Regression models for ordinal data. *Journal of the Royal Statistical Society: Series B (Methodological)*, 42(2):109–127.
- McCullagh, P. and Nelder, J. A. (1989). *Generalized Linear Models, Vol. 37 of Monographs on Statistics and Applied Probability*. Chapman and Hall, London.
- Murray, J. S. (2017). Log-linear Bayesian additive regression trees for categorical and count responses. *arXiv preprint arXiv:1701.01503*.
- Neal, R. M. (2003). Slice sampling. *Annals of Statistics*, pages 705–741.
- Neelon, B. et al. (2019). Bayesian zero-inflated negative binomial regression based on pólya-gamma mixtures. *Bayesian Analysis*, 14(3):849–875.
- O’Hara, R. B. and Kotze, D. J. (2010). Do not log-transform count data. *Methods in Ecology and Evolution*, 1(2):118–122.
- Osthus, D., Gattiker, J., Friedhorsky, R., and Del Valle, S. Y. (2018). Dynamic Bayesian influenza forecasting in the United States with hierarchical discrepancy. *Bayesian Analysis*.
- Polson, N. G., Scott, J. G., and Windle, J. (2013). Bayesian inference for logistic models using Pólya–Gamma latent variables. *Journal of the American Statistical Association*, 108(504):1339–1349.

- Ramsay, J. O. (1988). Monotone regression splines in action. *Statistical science*, 3(4):425–441.
- Rue, H. (2001). Fast sampling of Gaussian Markov random fields. *Journal of the Royal Statistical Society: Series B (Statistical Methodology)*, 63(2):325–338.
- Sellers, K. F. and Shmueli, G. (2010). A flexible regression model for count data. *The Annals of Applied Statistics*, pages 943–961.
- Shen, H. and Huang, J. Z. (2008). Interday forecasting and intraday updating of call center arrivals. *Manufacturing & Service Operations Management*, 10(3):391–410.
- Vihola, M. (2012). Robust adaptive metropolis algorithm with coerced acceptance rate. *Statistics and Computing*, 22(5):997–1008.
- Wand, M. and Ormerod, J. (2008). On semiparametric regression with O’Sullivan penalized splines. *Australian & New Zealand Journal of Statistics*, 50(2):179–198.
- Wang, W. and Yan, J. (2018). *splines2: Regression Spline Functions and Classes*. R package version 0.2.8.
- Warton, D. I. (2018). Why you cannot transform your way out of trouble for small counts. *Biometrics*, 74(1):362–368.
- Watanabe, S. (2010). Asymptotic equivalence of Bayes cross validation and widely applicable information criterion in singular learning theory. *Journal of Machine Learning Research*, 11(Dec):3571–3594.
- Wood, S. (2006). *Generalized additive models: an introduction with R*. CRC press.
- Zhou, M., Li, L., Dunson, D., and Carin, L. (2012). Lognormal and gamma mixed negative binomial regression. In *Proceedings of the International Conference on Machine Learning*, volume 2012, page 1343. NIH Public Access.